RESEARCH ARTICLE • OPEN ACCESS

A dynamical analysis of a predator-prey model: Exploring the influence of the Allee effect, environmental protection, and supplementary food sources

Resmawan Resmawan, Agus Suryanto, Isnani Darti, and Hasan S. Panigoro

Volume 6, Issue 4, Pages 311–328, December 2025

Received 16 June 2025, Revised 18 November 2025, Accepted 30 November 2025, Published Online 3 December 2025

To Cite this Article : R. Resmawan, A. Suryanto, I. Darti, and H. S. Panigoro,"A dynamical analysis of a predator-prey model: Exploring the influence of the Allee effect, environmental protection, and supplementary food sources", *Jambura J. Biomath*, vol. 6, no. 4, pp. 311–328, 2025, *https://doi.org/10.37905/jjbm.v6i4.32685*

JOURNAL INFO • JAMBURA JOURNAL OF BIOMATHEMATICS

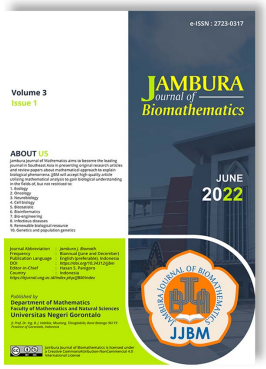

Homepage	:	http://ejurnal.ung.ac.id/index.php/JJBM/index
Journal Abbreviation	:	Jambura J. Biomath.
Frequency	:	Quarterly (March, June, September and December)
Publication Language	:	English
DOI	:	https://doi.org/10.37905/jjbm
Online ISSN	:	2723-0317
Editor-in-Chief	:	Hasan S. Panigoro
Publisher	:	Department of Mathematics, Universitas Negeri Gorontalo
Country	:	Indonesia
OAI Address	:	http://ejurnal.ung.ac.id/index.php/jjbm/oai
Google Scholar ID	:	XzYgeKQAAAAJ
Email	:	editorial.jjbm@ung.ac.id

JAMBURA JOURNAL • FIND OUR OTHER JOURNALS

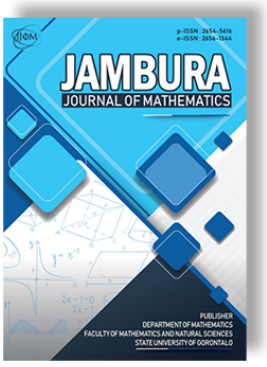

Jambura Journal of Mathematics

Jambura Journal of Mathematics Education

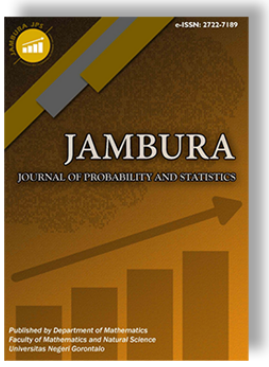

Jambura Journal of Probability and Statistics

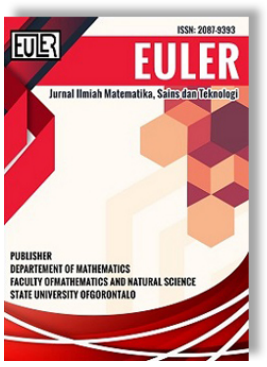

EULER : Jurnal Ilmiah Matematika, Sains, dan Teknologi

Jambura Journal of Biomathematics, Volume 6, Issue 4, Pages 311–328, December 2025 https://doi.org/10.37905/jjbm.v6i4.32685

Research Article

Check for updates

A dynamical analysis of a predator-prey model: Exploring the influence of the Allee effect, environmental protection, and supplementary food sources

Resmawan Resmawan[1], **Agus Suryanto**[1,*], **Isnani Darti**[1], **and Hasan S. Panigoro**[2]

[1]*Department of Mathematics, University of Brawijaya, Malang City, East Java 65145, Indonesia*
[2]*Department of Mathematics, Universitas Negeri Gorontalo, Bone Bolango Regency, Gorontalo 96554, Indonesia*

ARTICLE HISTORY
Received 16 June 2025
Revised 18 November 2025
Accepted 30 November 2025
Published 3 December 2025

KEYWORDS
Allee effect
Forward bifurcation
Hopf bifurcation
Supplementary food
Environmental protection
Bistability

ABSTRACT. *This paper introduces a new predator-prey model with supplementary food sorces for the predator and the Allee effect on prey. Analytical proof of the existence, uniqueness, non-negativity, and boundedness of the solutions validates the model. Three equilibrium points are found: a trivial point, whose local stability depends on the Allee effect's strength; a semi-trivial point, and an interior point whose local stability depends on certain conditions. The Lyapunov function and La Salle invariance principle show that each equilibrium point is globally asymptotically stable. The system displays intricate dynamical behaviors, including forward and Hopf bifurcations, along with bistability, which is regulated by critical parameters such as the predation conversion rate, environmental protection rate, and supplementary food sources. Under a weak Allee effect, increasing the predation conversion rate or supplementary food can shift the system from predator extinction to oscillatory coexistence. In contrast, under a strong Allee effect, these increases may instead drive both species to extinction if thresholds are exceeded. Moreover, variations in environmental protection rate yield contrasting outcomes: while a higher rate under weak Allee conditions may stabilize prey and eliminate predators, under strong Allee conditions, it may lead to total extinction. These findings illustrate the intricate relationship between biological and environmental components, highlighting the necessity for preventive measures and supplementary resources in population outcomes. The findings indicate that environmental protection and supplementary food sources influence species persistence and extinction in predator-prey dynamics, which is crucial for ecological conservation.*

1. Introduction

Predator-prey relationships as a fundamental topic in mathematical ecology have been extensively investigated to understand population dynamics in ecosystems. Mathematical modeling as the main tool describing this relationship allows scientists to project the survival of species through time, taking into account various ecological factors that affect their interactions. The interaction between two interdependent species can be analyzed through conventional predator-prey models, especially those developed by Lotka [1] and Volterra [2]. The classic Lotka-Volterra model has undergone several modifications, including the integration of a logistic growth function for the prey population, which became known as the Gause model [3]. However, these models are often considered too simple as they ignore more complicated ecological factors. Therefore, many modifications were made involving various functional responses [4, 5]. Holling identified three main types of functional responses based on prey population dynamics (Holling types I, II, and III), which have been widely used in ecological studies [6, 7]. Furthermore, ratio-dependent models like Beddington-DeAngelis and Crowley-Martin as well as Monod-Haldane and other functional responses have been created to enhance knowledge of species interactions in ecosystems [8–10]. Moreover, ecological elements such as the Allee effect and the accessibility of supplementary food for predators also influence predator-prey interactions. These elements taken together can increase the complexity of predator-prey interactions and reflect a key emphasis in modern ecological studies.

The Allee effect has been a focus of research in mathematical ecology over the past few decades, with many recent studies demonstrating the significance of this effect in understanding population dynamics. This phenomenon describes a situation where prey populations experience reduced growth rates when the number of individuals is too low, which can be caused by difficulties in finding mates, group protection, or cooperation in finding food [11]. The use of the Allee effect in predator-prey models has garnered considerable focus. Rahmi et al. [12] examined stability within a fractional-order Leslie-Gower model incorporating Allee effects in predators, demonstrating its influence on species stability. Panigoro and Rahmi [13, 14] created a Lotka-Volterra model with additive Allee effects, elucidating the difficulties predators encounter amid fluctuations in prey populations. Rahmi et al. [15] modified the Leslie-Gower model to

*Corresponding Author.

Email : *suryanto@ub.ac.id* (A. Suryanto)
Homepage : http://ejurnal.ung.ac.id/index.php/JJBM/index / E-ISSN : 2723-0317

combine the Beddington-DeAngelis functional response with the double Allee effect and memory. Anggriani et al. [16] incorporated the aspect of intraspecific rivalry inside the framework of the Allee effect, illustrating more authentic predator behavior. These studies jointly underscore the significance of comprehending the Allee effect's impact and establish a foundation for subsequent research on predator-prey dynamics. Recent research has shown that including the Allee effect in predator-prey models creates far more complex dynamics, such as bistability, local extinction, and increased risk of prey population extinction [17–21]. Investigations into variations in Allee effects show that prey populations with Allee thresholds exhibit differences in the stability and complexity of dynamic behavior [22–25]. Furthermore, issues such as predation uncertainty and the effect of group behavior on prey populations have started to be addressed [26, 27]. Despite several studies, the majority inadequately depict the interplay between the Allee effect and other ecological factors. Additional research incorporating the Allee effect alongside diverse ecological responses-such as supplementary food sources and behavioral impacts is essential to provide a comprehensive understanding of predator-prey dynamics in complex systems.

Another essential factor that significantly impacts predator-prey dynamics is the accessibility of supplementary food sources for predators. Providing supplementary food to predators alleviates predation pressure on primary prey species, enhancing ecosystem stability [28]. Multiple studies have incorporated supplementary food into predator-prey models, underscoring its substantial impact on the stability and intricacy of population dynamics. Supplemental food can modify predator-prey dynamics, stabilizing certain situations [29] while inducing fluctuations that may lead to extinction in others [30]. Debnath et al. [29] illustrated in a fractional differential model that the provision of food enhances biological control and stabilizes predator-prey dynamics. Meanwhile, Gökçe [30] showed that supplementary food can produce Hopf bifurcations, which make predator and prey populations oscillate. Furthermore, recent research has focused more specifically on examining the impact of various supplementary food sources. Prasad et al. [31] emphasized the significance of supplementary food in influencing population dynamics, while García & Cuenca [32] examined the impact of supplementary food sources on predator diets utilizing the Leslie-Gower model. Saha et al. [33] investigated the effects of supplementary food in conjunction with prey protection, whereas Mondal and Samanta [34] found that supplementary food doesn't necessarily help predators develop and may even lower predator biomass, depending on the amount consumed and the system's structure. Wang et al. [35] explored the correlation between supplementary food sources and protective mechanisms in the spatiotemporal dynamics of predator-prey interactions, whereas Singh and Poonam [36] discovered that supplementary food could trigger phase transitions in predator-prey systems. Many studies, however, neglect the impact of the Allee effect, which may obfuscate the interactions between predators and prey. Therefore, additional study is required to incorporate the Allee effect with the supplementary food dimension in predator-prey models to improve understanding of complex ecosystem dynamics.

To date, the integration of the Allee effect and supplementary food within predator-prey models remains markedly underexplored. Nevertheless, the interaction between these two ecological mechanisms can generate unexpected and complex dynamics, complicating the assessment of population stability. The scant research regarding their synergistic effects constrains the current comprehension of the nonlinear interactions that may emerge, encompassing modified extinction thresholds, significant bifurcation structures, and transitions in the stability regime of predator-prey systems. This gap underscores the need for a comprehensive mathematical framework to examine the synergistic effects of these interacting factors rigorously.

This study addresses this gap by proposing and analyzing a novel predator–prey model that integrates a modified Holling Type II functional response, accounting for supplementary food; logistic growth of the prey population, incorporating an additive Allee effect; and the impact of supplementary food availability on the predator's consumption and survival dynamics.

From a methodological standpoint, the study employs local and global stability analyses to determine the existence and nature of equilibrium points under varying ecological conditions. These analyses are conducted within a multidimensional parameter space that includes the Allee effect strength, predation conversion rate, quantity of supplementary food for predators, and environmental protection rate. To explore dynamic transitions within the system, bifurcation analysis, with an emphasis on Hopf bifurcations, is used to detect the onset of limit cycles and transitions from stable equilibrium points to oscillatory regimes. Furthermore, advanced tools such as eigenvalue analysis and Lyapunov function construction are utilized to examine the behavior of trajectories near equilibrium points and to characterize the system's response to perturbations.

Complementing the analytical results, numerical simulations using the fourth-order Runge-Kutta method are conducted to visualize the system's long-term behavior across diverse ecological scenarios. These simulations reveal critical insights into the emergence of oscillatory dynamics, sudden population collapses, and stabilization phenomena. They highlight that higher Allee thresholds, when combined with excessive supplementary food, may paradoxically destabilize the system, counteracting initial assumptions about their stabilizing roles.

In summary, this research makes several significant theoretical contributions to the field of mathematical ecology by:

1. Introducing a novel modeling framework to study the coupled influence of the Allee effect and supplementary food on predator-prey dynamics;
2. Identifying critical thresholds and bifurcation conditions that govern shifts in system behavior; and
3. Providing ecological interpretations of the model outcomes that can inform population management and conservation strategies, especially for species susceptible to extinction due to low-density effects and predation pressure.

The findings are anticipated to not only advance the theoretical landscape of predator-prey modeling but also serve as a foundation for policy-relevant recommendations in biodiversity conservation, particularly in contexts where anthropogenic interventions, such as food provisioning, interact with intrinsic species vulnerabilities.

Table 1. Model parameters, definitions, and dimensional units.

Parameter	Definition	Dimension
r	Intrinsic growth rate of the prey	time^{-1}
K	Environmental carrying capacity of the prey	density
h	Severity of the Allee effect	density
w	Scaling parameter of the Allee effect	density
a	Maximum predation rate	time^{-1}
b	Predation half-saturation constant	density
c	Biomass conversion efficiency	time^{-1}
δ	Natural mortality rate of predators	time^{-1}
k	Ratio of handling times (supplementary food vs prey)	dimensionless
m	Predator efficiency in locating supplementary food	dimensionless
A	Quantity of supplementary food available to predators	density

2. Model Development

This section presents a predator-prey model that integrates the Allee effect on prey and the provision of supplementary food for predators. The model is based on previous research: Bai and Zhang [37] suggested that the Allee effect may hinder the growth of prey populations at low densities. Conversely, Debnath et al. [29] showed that supplementary food can alleviate predation pressure and alter predator behavior. The predator-prey interaction incorporating an Allee effect in the prey population and the influence of supplementary food for predators is described by the following system of differential equations:

$$\begin{aligned} \frac{dN}{dt} &= rN\left(1-\frac{N}{K}-\frac{h}{w+N}\right)-\frac{aNP}{b+kmA+N}, \\ \frac{dP}{dt} &= \frac{c(N+mA)P}{b+kmA+N}-\delta P, \end{aligned} \tag{1}$$

where $N(t)$ and $P(t)$ denote the prey and predator densities, respectively. All parameters are positive, and their definitions and dimensional units are summarized in Table 1.

The prey population $N(t)$ follows logistic growth with intrinsic rate r and carrying capacity K, but is additionally influenced by an Allee effect captured by parameters h and w. The Allee effect accounts for reduced reproductive success or survival at low prey densities, arising from mechanisms such as difficulty in finding mates, diminished cooperative defense, or increased susceptibility to predation. When the prey density falls below the threshold determined by h and w, its growth rate declines, increasing the risk of population collapse. In this context, the term rh appearing in the expression

$$rN\left(1-\frac{N}{K}-\frac{h}{w+N}\right)$$

represents the maximal reduction in the prey per-capita growth rate due to the Allee effect when prey density is close to zero. Biologically, rh represents the strength of the negative demographic pressure experienced by the prey population at very low densities, combining both the intrinsic rate capacity r and the severity of the Allee effect h.

Predation follows a modified Holling-type II functional response that depends on both prey density and the availability of supplementary food. The parameter a specifies the maximum predation rate, while the half-saturation constant b determines the prey density at which predation reaches half of this maximum. The parameters k, m, and A govern how supplementary food modifies predator foraging behavior: k scales the relative handling time, m measures the predator's ability to locate supplementary food, and A represents the quantity of supplementary food provided.

The predator population $P(t)$ grows through the consumption of prey and supplementary food, with conversion efficiency determined by parameter c. Natural mortality occurs at rate δ. Overall, the model incorporates the main ecological processes governing the system, including density-dependent prey growth, nonlinear predation, and the influence of supplementary food, which can either stabilize or destabilize predator persistence.

3. Existence and Uniqueness

Theorem 1. *Let $M > 0$ be a constant satisfying $M = \max\{N, P\}$. For each non-negative initial condition on Ω, the model (1) has a unique solution on $\Omega \times [0, T_+]$ for some finite time $T_+ < \infty$.*

Proof. The existence and uniqueness of the model's (1) solution will be proved in $\Omega \times [0, T]$ with $T < \infty$. Let $X = (N, P)$ and $\bar{X} = (\bar{N}, \bar{P})$, with the mapping $F(X) = (F_1(X), F_2(X))$ and

$$\begin{aligned} F_1(X) &= rN\left(1-\frac{N}{K}-\frac{h}{w+N}\right)-\frac{aNP}{b+kmA+N}, \\ F_2(X) &= \frac{c(N+mA)P}{b+kmA+N}-\delta P. \end{aligned} \tag{2}$$

For every $X,\ \bar{X} \in \Omega$, it holds that

$$\begin{aligned} \|F(X)-F(\bar{X})\| &= |F_1(X)-F_1(\bar{X})|+|F_2(X)-F_2(\bar{X})|, \\ &= \left|\left[rN\left(1-\frac{N}{K}-\frac{h}{w+N}\right)-\frac{aNP}{b+kmA+N}\right]\right. \\ &\quad \left.-\left[r\bar{N}\left(1-\frac{\bar{N}}{K}-\frac{h}{w+\bar{N}}\right)-\frac{a\bar{N}\bar{P}}{b+kmA+\bar{N}}\right]\right| \\ &\quad +\left|\left[\frac{c(N+mA)P}{b+kmA+N}-\delta P\right]-\left[\frac{c(\bar{N}+mA)\bar{P}}{b+kmA+\bar{N}}\right.\right. \\ &\quad \left.\left.-\delta\bar{P}\right]\right|, \\ &\leq |r(N-\bar{N})|+\left|\frac{r}{K}(N^2-\bar{N}^2)\right|+\left|\frac{hrw(N-\bar{N})}{(w+N)(w+\bar{N})}\right| \\ &\quad +\left|a\left(\frac{(b+kmA)(N(P-\bar{P})+\bar{P}(N-\bar{N}))}{(b+kmA+N)(b+kmA+\bar{N})}\right.\right. \end{aligned}$$

$$
\begin{aligned}
&+\frac{\bar{N}N(P-\bar{P})}{(b+kmA+N)(b+kmA+\bar{N})}\Bigg)\Bigg|\\
&+\left|c\left(\frac{(b+kmA)(N(P-\bar{P})+\bar{P}(N-\bar{N}))}{(b+kmA+N)(b+kmA+\bar{N})}\right.\right.\\
&\left.\left.+\frac{\bar{N}N(P-\bar{P})+mA\bar{N}(P-\bar{P})}{(b+kmA+N)(b+kmA+\bar{N})}\right)\right|\\
&+\left|\frac{cmA\bar{P}(N-\bar{N})}{(b+kmA+N)(b+kmA+\bar{N})}\right|\\
&+\left|\frac{c(bmA+km^2A^2)(P-\bar{P})}{(b+kmA+N)(b+kmA+\bar{N})}\right|\\
&+\left|\delta(P-\bar{P})\right|,\\
=&\left(r+\frac{r}{K}\left|N+\bar{N}\right|+\frac{hrw}{(w+N)(w+\bar{N})}\right.\\
&+\frac{a(b+kmA)\bar{P}}{(b+kmA+N)(b+kmA+\bar{N})}\\
&+\frac{c(b+kmA)\bar{P}}{(b+kmA+N)(b+kmA+\bar{N})}\\
&\left.+\frac{cmA\bar{P}}{(b+kmA+N)(b+kmA+\bar{N})}\right)\left|N-\bar{N}\right|\\
&+\left(\frac{aN(b+kmA+\bar{N})}{(b+kmA+N)(b+kmA+\bar{N})}\right.\\
&+\frac{c((b+kmA)N+\bar{N}N+mA\bar{N})}{(b+kmA+N)(b+kmA+\bar{N})}\\
&\left.+\frac{c(bmA+km^2A^2)}{(b+kmA+N)(b+kmA+\bar{N})}+\delta\right)\left|P-\bar{P}\right|.
\end{aligned}
\tag{3}
$$

Next, let M be a positive constant with $M=\max\{N,P\}$, such that inequality (3) can be written as

$$
\begin{aligned}
\left\|F(X)-F(\bar{X})\right\| \leq &\left(r+\frac{2rM}{K}+\frac{hrw}{(w+M)^2}+\frac{a(b+kmA)M}{(b+kmA+M)^2}\right.\\
&\left.+\frac{c(b+kmA)M}{(b+kmA+M)^2}+\frac{cmAM}{(b+kmA+M)^2}\right)\left|N-\bar{N}\right|\\
&+\left(\frac{aM(b+kmA+M)}{(b+kmA+M)^2}+\frac{c(bmA+km^2A^2)}{(b+kmA+M)^2}\right.\\
&\left.+\frac{c((b+kmA)M+M^2+mAM)}{(b+kmA+M)^2}+\delta\right)\left|P-\bar{P}\right|\\
=&\,L_1\left|N-\bar{N}\right|+L_2\left|P-\bar{P}\right|,
\end{aligned}
$$

with

$$
\begin{aligned}
L_1&=r+\frac{2rM}{K}+\frac{hrw}{(w+M)^2}+\frac{M(a+c)(b+kmA)+cmAM}{(b+kmA+M)^2},\\
L_2&=\delta+\frac{(a+c)M+cmA}{b+kmA+M}.
\end{aligned}
$$

By choosing a positive constant $L=\max(L_1,L_2)$, we obtain

$$
\begin{aligned}
\left\|F(X)-F(\bar{X})\right\|&=L\left(\left|(N-\bar{N})\right|+\left|(P-\bar{P})\right|\right)\\
&\leq L\left\|X-\bar{X}\right\|.
\end{aligned}
$$

According to the Lipschitz condition [38], the function $F(X)$ satisfies the Lipschitz condition criteria, ensuring the existence of a unique solution $X(t)$ of the model (1) with initial value $X(0)=(N(0),P(0))\in\Omega$. Therefore, the solution of the model (1) exists and is unique. □

4. Nonnegativity and Boundedness

Theorem 2. *All solution of the model (1) with positive initial values $(N(0),P(0))\in\mathbb{R}^2_+$ are always non-negative.*

Proof. We will prove that if $(N(0),P(0))\in\mathbb{R}^2_+$, then $N(t)\geq 0$ and $N(t)\geq 0, \forall t\geq 0$. For the first case, we will prove $N(t)\geq 0$. Assume that $N(t)\geq 0,\ \forall t\geq 0$ is not true. There is $t_1>0$ such that

$$
\begin{cases}
N(t)>0, & 0<t<t_1\\
N(t)=0, & t=t_1\\
N(t)<0, & t>t_1.
\end{cases}
$$

If $N(t_1)=0$, we can use the first equation in the model (1) to obtain

$$
\left.\frac{dN}{dt}\right|_{t=t_1}=0.
$$

Thus, there is no change in population density at $t=t_1$. This contradicts the statement that $N(t)<0$ for $t>t_1$, such that the previous assumption is false. It means the statement that $N(t)\geq 0,\ \forall t\geq 0$ is true. In the same way, it can be shown that $P(t)\geq 0,\ \forall t\geq 0$. □

Theorem 3. *All solutions of the model (1) with initial values $(N(0),P(0))\in\mathbb{R}^2_+$ are uniformly bounded in $\Omega=\left\{(N,P)\in R^2_+ : 0<Q\leq\frac{K(r+\gamma)^2}{4\gamma r}+\varepsilon,\ \varepsilon>0\right\}$.*

Proof. Define

$$
Q=N+\frac{a}{c}P.
$$

For any $\gamma>0$, it can be shown that,

$$
\begin{aligned}
\frac{dQ}{dt}+\gamma Q&=rN\left(1-\frac{N}{K}-\frac{h}{w+N}\right)-\frac{aNP}{b+kmA+N}\\
&\quad+\frac{a}{c}\left(\frac{c(N+mA)P}{b+kmA+N}-\delta P\right)+\gamma N+\frac{\gamma a}{c}P\\
&\leq\frac{K(r+\gamma)^2}{4r}+\frac{amAP}{kmA}-\frac{\delta a}{c}P+\frac{\gamma a}{c}P\\
&=\frac{K(r+\gamma)^2}{4r}+\frac{\gamma k-(\delta k-c)}{kc}aP.
\end{aligned}
$$

By choosing a sufficiently small γ that satisfies $\gamma k<(\delta k-c)$, we obtain:

$$
\frac{dQ}{dt}+\gamma Q\leq\frac{K(r+\gamma)^2}{4r}.
$$

Based on Gronwall's inequality [39], we have

$$
\lim_{t\to\infty}Q(t)\leq\frac{K(r+\gamma)^2}{4\gamma r}.
$$

This shows that $Q(t)$ are bounded in Ω, i.e.

$$
\Omega=\left\{(N,P)\in R^2_+ : 0<Q\leq\frac{K(r+\gamma)^2}{4\gamma r}+\varepsilon,\ \varepsilon>0\right\}.
$$

□

5. Existence and Stability of Equilibrium Points

5.1. The Existence of Equilibrium Points

Clearly, $E_0(0,0)$ consistently serves as an equilibrium point of the model (1). For any nonnegative equilibrium $E(N,P)$ of the model (1), its components must comply with the following equations:

$$N\left[r\left(1-\frac{N}{K}-\frac{h}{w+N}\right)-\frac{aP}{b+kmA+N}\right]=0, \quad (4)$$

$$P\left[\frac{c(N+mA)P}{b+kmA+N}-\delta\right]=0. \quad (5)$$

If $N=0$ and $P=0$, model (1) has only the trivial point $E_0(0,0)$. In the following, we discuss the scenario when $P=0$ and $N\neq 0$, i.e. the nonzero part of eq. (4), which results in

$$N_1=\frac{(K-w)+\sqrt{(K-w)^2-4K(h-w)}}{2},$$
$$N_2=\frac{(K-w)-\sqrt{(K-w)^2-4K(h-w)}}{2}.$$

The existence of N depends on the Allee effect condition $(h-w)$, the value of $K-w$, and $(K-w)^2-4K(h-w)$. As a consequence, we need to consider the following cases.

- Weak Allee Effect Case
  Let $\mathcal{D}=(K-w)^2-4K(h-w)$. The weak Allee effect in the model (1) occurs if $w>h$. If $w>h$, then $\mathcal{D}>0$, which leads to the existence of semi-trivial points depending on the value of $(K-w)$:
  a. If $w<K$, then $\sqrt{\mathcal{D}}>(K-w)$, so that $N_1>0$ and $N_2<0$.
  b. If $w>K$, then $\sqrt{\mathcal{D}}>(w-K)$, so that $N_1>0$ and $N_2<0$.
  Hence, if there is a weak Allee effect in the model (1), then there exists one semi-trivial point, namely $E_1(N_1,0)$.
- Strong Allee Effect Case
  The strong Allee effect in the model (1) occurs if $w<h$. If $w<h$, then the existence of semi-trivial points depends on $\mathcal{D}$ and $(K-w)$ value:
  a. If $\mathcal{D}<0$, then the semi-trivial point $E(N,0)$ do not exist.
  b. If $\mathcal{D}>0$, then $h<\frac{(K+w)^2}{4K}$. Furthermore, the existence of the semi-trivial point depends on $(K-w)$ value:
  (i) If $w<K$, then $\sqrt{\mathcal{D}}<(K-w)$, so that $N_1>0$ and $N_2>0$. In this case, there are two existing semi-trivial points, namely $E_1(N_1,0)$ and $E_2(N_2,0)$.
  (ii) If $w>K$, also $\sqrt{\mathcal{D}}<(K-w)$, so that $N_1<0$ and $N_2<0$. In this case, $E(N,0)$ do not exist.
  c. If $\mathcal{D}=0$, then there exists one existing semi-trivial point, i.e $E_3(N_3,0)$, with $N_3=\frac{K-w}{2}$. E_3 exists if $K>w$ and do not exist if $K<w$.

Therefore, there are three semi-trivial points, namely $E_1(N_1,0)$, $E_2(N_2,0)$, and $E_3(N_3,0)$, whose existency depends on the Allee effect conditions. Now, we summarise our analysis in the following theorem.

Theorem 4. *Suppose $\Psi=K-w$ and $\Phi=h-w$. The model (1) has the following equilibrium points:*
(i) The trivial equilibrium point, denoted as $E_0(0,0)$, which always exists in R^2_+.
(ii) Let $N_1=\frac{\Psi+\sqrt{\Psi^2-4K\Phi}}{2}$. If $w>h$ (weak Allee effect), then the semi-trivial equilibrium point, $E_1(N_1,0)$, exists and is unique.
(iii) Let $\Pi=K+w$, $K>w$, $N_2=\frac{\Psi-\sqrt{\Psi^2-4K\Phi}}{2}$, $N_3=\frac{\Psi}{2}$, and $w<h$ (strong Allee effect):
(a) If $h=\frac{\Pi^2}{4K}$, then the semi-trivial equilibrium point, $E_3(N_3,0)$, exists and is unique.
(b) If $h<\frac{\Pi^2}{4K}$, then two semi-trivial equilibrium points exist, which are $E_1(N_1,0)$ and $E_2(N_2,0)$.

Furthermore, we discuss the scenario when $N\neq 0$ and $P\neq 0$, that is the condition in eqs. (4) and (5). From eq. (5), provided that $P\neq 0$, we obtain:

$$N_4=\frac{\delta b+\delta kmA-cmA}{c-\delta}, \text{ with } c-\delta\neq 0.$$

Therefore, we need to consider the following cases.

- If $c>\delta$, it must to be shown that $\delta b+\delta kmA-cmA>0$, which only satisfies if $\frac{\delta b}{mA}+\delta k>c$. Thus, $N_4>0$ under the condition $\delta<c<\frac{\delta b}{mA}+\delta k$, if $c-\delta>0$.
- If $c<\delta$, it must be shown that $\delta b+\delta kmA-cmA<0$, which only satisfies if $\frac{\delta b}{mA}+\delta k<c$. Thus, $N_4>0$ under the condition $\frac{\delta b}{mA}+\delta k<c<\delta$, if $c-\delta<0$.

From eq. (4), provided that $N\neq 0$, we obtain:

$$P_4=\frac{r(b+kmA+N_4)\left[(K-w)N_4-K(h-w)-N_4^2\right]}{Ka(w+N_4)}.$$

Thus, $P_4>0$ under the condition $(K-w)N_4-K(h-w)-N_4^2>0$.
Now, we summarise our analysis in the following theorem.

Theorem 5. *Suppose $N_4=\frac{\delta(b+kmA)-cmA}{c-\delta}$ and $P_4=\frac{r(b+kmA+N_4)\left[(K-w)N_4-K(h-w)-N_4^2\right]}{Ka(w+N_4)}$. The interior equilibrium point $E_4(N_4,P_4)$, exists if the following conditions are satisfied:*
(i) $(K-w)N_4-K(h-w)-N_4^2>0$,
(ii) If $c>\delta$, then $\delta<c<\delta\left(\frac{b}{mA}+k\right)$,
(iii) If $c<\delta$, then $\delta\left(\frac{b}{mA}+k\right)<c<\delta$.

5.2. Local Stability of Equilibrium Points

The model (1) is linearized around the equilibrium point to assess local stability. The linear aspect of this linearized model is known as the Jacobian matrix. The eigenvalues of the Jacobian matrix are used to evaluate the stability of equilibrium points [40]. Linearization around the equilibrium point yields the Jacobian matrix:

$$J=\begin{bmatrix} r-\frac{2r}{K}N-\frac{rhw}{(w+N)^2}-\frac{aP(b+kmA)}{(b+kmA+N)^2} & -\frac{aN}{b+kmA+N} \\ \frac{(b+kmA-mA)cP}{(b+kmA+N)^2} & \frac{c(N+mA)}{b+kmA+N}-\delta \end{bmatrix}. \quad (6)$$

According to the Jacobian matrix (6), the equilibrium point's stability is established in the subsequent theorems.

Theorem 6. *Let $c < \frac{\delta b}{mA} + \delta k$. The trivial equilibrium point, $E_0\,(0,0)$, is L.A.S if the Allee effect is strong $(w < h)$ and unstable if the Allee effect is weak $(w > h)$.*

Proof. By substituting E_0 to Jacobian matrix (6), we obtain:

$$J_{E_0} = \begin{bmatrix} \frac{r(w-h)}{w} & 0 \\ 0 & \frac{cmA}{b+kmA} - \delta \end{bmatrix},$$

and we get two eigen values $\lambda_1 = \frac{r(w-h)}{w}$ and $\lambda_2 = \frac{cmA-\delta(b+kmA)}{b+kmA}$. It can be shown that $\lambda_1 < 0$ if $w < h$, while $\lambda_2 < 0$ if $c < \frac{\delta b}{mA} + \delta k$. Thus, E_0 is L.A.S if $w < h$ (strong Allee effect) and $c < \frac{\delta b}{mA} + \delta k$, and unstable otherwise. □

Theorem 7. *The local stability of the semi-trivial equilibrium points $E_0(N_n, 0)$, where $n = 1, 2, 3$ of the model (1) is described by the following statement:*

(i) Suppose $w > h$ (weak Allee effect). E_1 is L.A.S if $c < \frac{\delta(b+kmA+N_1)}{mA+N_1}$ and unstable (saddle-node) if $c > \frac{\delta(b+kmA+N_1)}{mA+N_1}$.

(ii) Suppose $\Pi = K + w, w < K$, $c < \frac{\delta(b+kmA+N_n)}{mA+N_n}$ and $w < h$ (strong Allee effect):

(a) If $h = \frac{\Pi^2}{4K}$, then E_3 is non-hyperbolic.

(b) If $h < \frac{\Pi^2}{4K}$, then E_1 is L.A.S and E_2 is unstable (saddle-node).

Proof. By substituting E_n to Jacobian matrix (6), we obtain:

$$J_{E_n} = \begin{bmatrix} rN_n\left(\frac{h}{(w+N_n)^2} - \frac{1}{K}\right) & -\frac{aN_n}{b+kmA+N_n} \\ 0 & \frac{c(N_n+mA)-\delta(b+kmA+N_n)}{b+kmA+N_n} \end{bmatrix},$$

and we get two eigen values $\lambda_1 = rN_n\left(\frac{h}{(w+N_n)^2} - \frac{1}{K}\right)$ and $\lambda_2 = \frac{c(N_n+mA)-\delta(b+kmA+N_n)}{b+kmA+N_n}$. From the second eigenvalue, it can be shown that $\lambda_2 < 0$ if

$$c < \frac{\delta(b+kmA+N_n)}{mA+N_n}.$$

Subsequently, we need to examine the first eigenvalue condition in according to the Allee effect condition.

- Weak Allee effect case
  According to Theorem 4 (ii), $E_1(N_1, 0)$ is the only semi-trivial equilibrium point that exists under the weak Allee effect $(w > h)$. If $h < w$, then $(K-w)^2 - 4K(h-w) > 0$, which results in $h < \frac{(K+w)^2}{4K}$, so it can be shown that

  $$\lambda_1 < -\frac{rN_1(K+w)\sqrt{(K+w)^2 - 4Kh}}{2K(w+N_1^*)^2} < 0.$$

  Thus, E_1 is L.A.S if $c < \frac{\delta(b+kmA+N_1)}{mA+N_1}$ and unstable otherwise.

- Strong Allee effect case
  In accordance with Theorem 4 (iii), the stability of $E_n, n = 1, 2, 3$ must be demonstrated under the following conditions:
  - If $h = \frac{(K+w)^2}{4K}$, we obtain $\lambda_1 = 0$. Since one of the eigenvalues is zero, the semi-trivial equilibrium point $E_3 = \left(\frac{K-w}{2}, 0\right)$ is non-hyperbolic.
  - If $h < \frac{(K+w)^2}{4K}$, we obtain

    $$\lambda_1 = \frac{rN_{1,2}}{K}\left(\frac{(K+w)^2 - \left((K+w) \pm \sqrt{(K+w)^2 - 4Kh}\right)^2}{\left((K+w) \pm \sqrt{(K+w)^2 - 4Kh}\right)^2}\right).$$

    1. For E_1, we can show that $(K+w)^2 - \left((K+w) + \sqrt{(K+w)^2 - 4Kh}\right)^2 < -2(K+w)\sqrt{(K+w)^2 - 4Kh} < 0$. Consequently, we derive $\lambda_1 < 0$, indicating that E_1 is L.A.S.
    2. For E_2, we can show that $(K+w)^2 - \left((K+w) - \sqrt{(K+w)^2 - 4Kh}\right)^2 > 2(K+w)\sqrt{(K+w)^2 - 4Kh} > 0$. Consequently, we derive $\lambda_1 > 0$, indicating that E_2 is unstable.

□

Theorem 8. *Suppose $k > 1$ or $k < 1$ and $b > |(k-1)mA|$. Also, suppose $N_4 = \frac{\delta(b+kmA)-cmA}{c-\delta}$ and $P_4 = \frac{r(b+kmA+N_4)\left[(K-w)N_4 - K(h-w) - N_4^2\right]}{Ka(w+N_4)}$. The interior equilibrium point $E_4(N_4, P_4)$ of the model (1) is L.A.S if the following conditions are satisfied:*

(i) $Kh < (w+N_4)^2$,

(ii) $\left|Kh - (w+N_4)^2\right| > \frac{Ka(w+N_4)^2 P_4}{r(b+kmA+N_4)^2}$.

Proof. By substituting E_4 to Jacobian matrix (6), we obtain:

$$J_{E_4} = \begin{bmatrix} \left(\frac{Kh-(w+N_4)^2}{K(w+N_4)^2}\right) rN_4 + \frac{aN_4P_4}{(b+kmA+N_4)^2} & -\frac{aN_4}{b+kmA+N_4} \\ \frac{(b+kmA-mA)cP_4}{(b+kmA+N_4)^2} & 0 \end{bmatrix}, \tag{7}$$

with

$$N_4 = \frac{\delta(b+kmA) - cmA}{c-\delta},$$

$$P_4 = \frac{r(b+kmA+N_4)\left[(K-w)N_4 - K(h-w) - N_4^2\right]}{Ka(w+N_4)}.$$

From the Jacobian matrix (7), the determinant and trace of the matrix are obtained:

$$\det(J_{E_4}) = \frac{ac(b+(k-1)mA)N_4P_4}{(b+kmA+N_4)^3}, \tag{8}$$

$$\mathrm{tr}(J_{E_4}) = \left(\frac{Kh-(w+N_4)^2}{K(w+N_4)^2}\right) rN_4 + \frac{aN_4P_4}{(b+kmA+N_4)^2}. \tag{9}$$

Subsequently, it is essential to demonstrate that E_4 exhibits local asymptotic stability under the condition that $\det(J_{E_4}) > 0$ and $\mathrm{tr}(J_{E_4}) < 0$.

Based on the eq. (8), the subsequent conditions can be indicated:

- If $k > 1$, then $\det(J_{E_4}) > 0$.
- If $k < 1$ and $b > |(k-1)mA|$ then $\det(J_{E_4}) > 0$.

Based on the eq. (9), it can be shown that $\text{tr}(J_{E_4}) < 0$ if the following conditions are satisfied:

- $Kh < (w+N_4)^2$,
- $\left|Kh - (w+N_4)^2\right| > \frac{Ka(w+N_4)^2P_4}{r(b+kmA+N_4)^2}$.

Therefore, E_4 is locally asymptotically stable if the following conditions hold:

(i) $Kh < (w+N_4)^2$,
(ii) $\left|Kh - (w+N_4)^2\right| > \frac{Ka(w+N_4)^2P_4}{r(b+kmA+N_4)^2}$,
(iii) $k > 1$ or $k < 1$ and $b > |(k-1)mA|$.

□

5.3. Global Stability of Equilibrium Points

The criteria for the global stability of the trivial, semi-trivial, and interior equilibrium points are provided in Theorem 9, 10, and 11, respectively.

Theorem 9. *If $K < w < h$ (strong Allee effect) and $cmA < \delta(b+kmA)$, then the trivial equilibrium point $E_0(0,0)$ is G.A.S.*

Proof. The model (1) can be modified as:

$$\begin{aligned}\frac{dN}{dt} &= -rN\left(\frac{h-w}{w+N}\right) - \frac{rN^2(w-K)}{K(w+N)} - \frac{rN^3}{K(w+N)} \\ &\quad - \frac{aNP}{b+kmA+N}, \\ \frac{dP}{dt} &= \frac{cNP}{b+kmA+N} + \frac{cmAP}{b+kmA+N} - \delta P.\end{aligned} \tag{10}$$

Define the Lyapunov function as:

$$V_0(N,P) = N + \frac{a}{c}P. \tag{11}$$

The first-order derivative of V_0 is

$$\begin{aligned}\frac{dV_0}{dt} &= \frac{\partial V_0}{\partial N}\frac{dN}{dt} + \frac{\partial V_0}{\partial P}\frac{dP}{dt} \\ &= -rN\left(\frac{h-w}{w+N}\right) - rN^2\left(\frac{w-K}{K(w+N)}\right) \\ &\quad - \frac{rN^3}{K(w+N)} - aP\left(\frac{\delta(b+kmA)-cmA}{c(b+kmA+N)}\right) \\ &\quad - \frac{a\delta NP}{c(b+kmA+N)}.\end{aligned}$$

If $K < w < h$ (strong Allee effect) and $cmA < \delta(b+kmA)$, then $\frac{dV_0}{dt} < 0$. In addition, $\frac{dV_0}{dt} = 0$ if and only if $N = 0$ and $P = 0$. According to LaSalle's invariance principle [41], the equilibrium point E_0 is G.A.S. □

Theorem 10. *If $h < \frac{w^2}{K}$ and $c < \frac{\delta(b+kmA)}{N^*+mA}$, then the semi-trivial equilibrium point $E_n(N^*,0)$ is G.A.S.*

Proof. The model (1) can be modified as:

$$\begin{aligned}\frac{dN}{dt} &= N\left(\frac{rh(N-N^*)}{(w+N^*)(w+N)} - \frac{r(N-N^*)}{K} - \frac{aP}{b+kmA+N}\right), \\ \frac{dP}{dt} &= \frac{cNP}{b+kmA+N} + \frac{cmAP}{b+kmA+N} - \delta P.\end{aligned} \tag{12}$$

The Lyapunov function is defined as follows:

$$V_1(N,P) = \left(N - N^* - N^*\ln\frac{N}{N^*}\right) + \frac{a}{c}P. \tag{13}$$

Thus, we can obtain the first-order derivative of V_1 in the following:

$$\begin{aligned}\frac{dV_1}{dt} &= \frac{\partial V_1}{\partial N}\frac{dN}{dt} + \frac{\partial V_1}{\partial P}\frac{dP}{dt} \\ &= -\frac{r(N-N^*)^2}{K} + \frac{rh(N-N^*)^2}{(w+N^*)(w+N)} + \frac{aN^*P}{b+kmA+N} \\ &\quad - \frac{aP\left(\delta(b+kmA)-cmA\right)}{c(b+kmA+N)} - \frac{\delta aNP}{c(b+kmA+N)} \\ &\le -\frac{r(N-N^*)^2}{K} + \frac{rh(N-N^*)^2}{w^2} + \frac{aN^*P}{b+kmA+N} \\ &\quad - \frac{aP\left(\delta(b+kmA)-cmA\right)}{c(b+kmA+N)} - \frac{\delta aNP}{c(b+kmA+N)} \\ &= -r\left(\frac{1}{K} - \frac{h}{w^2}\right)(N-N^*)^2 - \frac{\delta aNP}{c(b+kmA+N)} \\ &\quad - \frac{aP\left(\delta(b+kmA)-c(N^*+mA)\right)}{c(b+kmA+N)}.\end{aligned}$$

If $h < \frac{w^2}{K}$ and $c < \frac{\delta(b+kmA)}{N^*+mA}$, then $\frac{dV_1}{dt} < 0$. Furthermore, $\frac{dV_1}{dt} = 0$ if and only if $N = N^*$ and $P = 0$. Based on LaSalle's invariance principle [41], E_n is G.A.S. □

Theorem 11. *Let M is a positive constant. If $K < \frac{2rw^2(b+kmA)^2}{2rh(b+kmA)^2+2aw^2M+aw^2(b+kmA)+c^2w^2(b+kmA+mA)M}$ and $\delta > \frac{2c(mA+M)(b+kmA)+cM(b+kmA+mA)+a(b+kmA)}{2(b+kmA)^2}$, then the interior equilibrium point, $E_i(N^*,P^*)$, is G.A.S.*

Proof. The model (1) can be modified as:

$$\begin{aligned}\frac{dN}{dt} &= N\Bigg(\frac{r(N^*-N)}{K} + \frac{rh(w+N)-rh(w+N^*)}{(w+N^*)(w+N)} \\ &\quad + \frac{aP^*(b+kmA+N)-aP(b+kmA+N^*)}{(b+kmA+N^*)(b+kmA+N)}\Bigg), \\ \frac{dP}{dt} &= \frac{c(N+mA)P}{b+kmA+N} - \frac{c(N^*+mA)P^*}{b+kmA+N^*} - \delta(P-P^*).\end{aligned} \tag{14}$$

Define the Lyapunov function as

$$V_2(N,P) = \left(N - N^* - N^*\ln\frac{N}{N^*}\right) + \frac{1}{2}(P-P^*)^2. \tag{15}$$

The first-order derivative of V_2 is

$$\frac{dV_2}{dt} = \frac{\partial V_2}{\partial N}\frac{dN}{dt} + \frac{\partial V_2}{\partial P}\frac{dP}{dt}.$$

$$
\begin{aligned}
&= -\frac{r(N-N^*)^2}{K} + \frac{rh(N-N^*)^2}{(w+N^*)(w+N)} \\
&\quad + \frac{aP(N-N^*)^2}{(b+kmA+N^*)(b+kmA+N)} \\
&\quad + \frac{(cmA+cN)(P-P^*)^2}{b+kmA+N} - \delta(P-P^*)^2 \\
&\quad + \frac{(bc+ckmA+cmA)P^*(N-N^*)(P-P^*)}{(b+kmA+N)(b+kmA+N^*)} \\
&\quad - \frac{a(N-N^*)(P-P^*)}{b+kmA+N^*} \\
&\leq -\frac{r(N-N^*)^2}{K} + \frac{rh(N-N^*)^2}{(w+N^*)(w+N)} \\
&\quad - \delta(P-P^*)^2 + \frac{a(P-P^*)^2}{2(b+kmA+N^*)} \\
&\quad + \frac{(cmA+cN)(P-P^*)^2}{b+kmA+N} + \frac{a(N-N^*)^2}{2(b+kmA+N^*)} \\
&\quad + \frac{aP(N-N^*)^2}{(b+kmA+N^*)(b+kmA+N)} \\
&\quad + \frac{(bc+ckmA+cmA)P^*(N-N^*)^2}{2(b+kmA+N)(b+kmA+N^*)} \\
&\quad + \frac{(bc+ckmA+cmA)P^*(P-P^*)^2}{2(b+kmA+N)(b+kmA+N^*)}.
\end{aligned}
$$

The solution of the model (1) is bounded, as according to Theorem 3. Therefore, let M be a positive constant such that $N^*, P^*, N, P \leq M$. Consequently, we obtain

$$
\begin{aligned}
\frac{dV_2}{dt} &\leq -\frac{r(N-N^*)^2}{K} + \frac{rh(N-N^*)^2}{(w+N^*)(w+N)} - \delta(P-P^*)^2 \\
&\quad + \frac{aM(N-N^*)^2}{(b+kmA+N^*)(b+kmA+N)} \\
&\quad + \frac{(cmA+cM)(P-P^*)^2}{b+kmA+N} \\
&\quad + \frac{(bc+ckmA+cmA)M(N-N^*)^2}{2(b+kmA+N)(b+kmA+N^*)} \\
&\quad + \frac{(bc+ckmA+cmA)M(P-P^*)^2}{2(b+kmA+N)(b+kmA+N^*)} \\
&\quad + \frac{a(N-N^*)^2}{2(b+kmA+N^*)} + \frac{a(P-P^*)^2}{2(b+kmA+N^*)} \\
&\leq -\frac{r(N-N^*)^2}{K} + \frac{rh(N-N^*)^2}{w^2} + \frac{aM(N-N^*)^2}{(b+kmA)^2} \\
&\quad + \frac{(cmA+cM)(P-P^*)^2}{b+kmA} - \delta(P-P^*)^2 \\
&\quad + \frac{(bc+ckmA+cmA)M(N-N^*)^2}{2(b+kmA)^2} \\
&\quad + \frac{a(N-N^*)^2}{2(b+kmA)} + \frac{a(P-P^*)^2}{2(b+kmA)} \\
&\quad + \frac{(bc+ckmA+cmA)M(P-P^*)^2}{2(b+kmA)^2} \\
&= \left(\frac{\eta_1}{\eta_2} - \frac{r}{K}\right)(N-N^*)^2 + (\zeta-\delta)(P-P^*)^2,
\end{aligned}
$$

with

$$
\begin{aligned}
\eta_1 &= 2rh(b+kmA)^2 + 2aw^2M + aw^2(b+kmA) \\
&\quad + cw^2(b+kmA+mA)M, \\
\eta_2 &= 2w^2(b+kmA)^2, \\
\zeta &= \frac{2c(mA+M)(b+kmA) + cM(b+kmA+mA)}{2(b+kmA)^2} \\
&\quad + \frac{a(b+kmA)}{2(b+kmA)^2}.
\end{aligned}
$$

If $K < \frac{r\eta_2}{\eta_1}$ and $\delta > \zeta$, then $\frac{dV_2}{dt} < 0$. Additionally, $\frac{dV_2}{dt} = 0$ if and only if $N = N^*$ and $P = P^*$. By using LaSalle's invariance principle [41], E_i is G.A.S. □

6. Bifurcation Analysis

6.1. Forward Bifurcation

Based on Theorem 7 (i), the semi-trivial equilibrium point $E_1(N_1, 0)$ is L.A.S if $c < \frac{\delta(b+kmA+N_1)}{mA+N_1}$ and unstable if $c > \frac{\delta(b+kmA+N_1)}{mA+N_1}$, with $N_1 = \frac{(K-w)+\sqrt{(K-w)^2-4K(h-w)}}{2}$. Furthermore, the Jacobian matrix for E_1 is obtain as

$$
J_{E_1} = \begin{bmatrix} rN_1\left(\frac{h}{(w+N_1)^2} - \frac{1}{K}\right) & -\frac{aN_1}{b+kmA+N_1} \\ 0 & \frac{c(mA+N_1)}{b+kmA+N_1} - \delta \end{bmatrix}. \tag{16}
$$

The Jacobian matrix (16) contains two eigenvalues, which are indentified as:

$$
\lambda_1 = rN_1\left(\frac{h}{(w+N_1)^2} - \frac{1}{K}\right) < 0 \text{ and } \lambda_2 = \frac{c(mA+N_1)}{b+kmA+N_1} - \delta.
$$

The existence of forward bifurcations is established in Theorem 12.

Theorem 12. *Let* $c^* = \frac{\delta(b+kmA+N_1)}{mA+N_1}$, *where* $N_1 = \frac{(K-w)+\sqrt{(K-w)^2-4K(h-w)}}{2}$. *A forward bifurcation occurs when* $c = c^*$.

Proof. Assume that $c^* = \frac{\delta(b+kmA+N_1)}{mA+N_1}$. The Jacobian matrix for the equilibrium point E_1 has negative one of its eigenvalues and the other eigenvalues are zero when $c = c^*$. By substituting c into the Jacobian matrix (16), we obtain

$$
J_{E_1}|_{c=c^*} = \begin{bmatrix} rN_1\left(\frac{h}{(w+N_1)^2} - \frac{1}{K}\right) & -\frac{aN_1}{b+kmA+N_1} \\ 0 & 0 \end{bmatrix}.
$$

Suppose the right eigenvector for zero eigenvalue is

$$
\vec{w} = \begin{bmatrix} w_1 \\ w_2 \end{bmatrix},
$$

which satisfies

$$
\begin{bmatrix} rN_1\left(\frac{h}{(w+N_1)^2} - \frac{1}{K}\right) & -\frac{aN_1}{b+kmA+N_1} \\ 0 & 0 \end{bmatrix} \begin{bmatrix} w_1 \\ w_2 \end{bmatrix} = \begin{bmatrix} 0 \\ 0 \end{bmatrix}.
$$

Thus, the right eigenvector for the zero eigenvalue can be written as

$$\begin{bmatrix} w_1 \\ w_2 \end{bmatrix} = \begin{bmatrix} 1 \\ \frac{r(b+kmA+N_1)}{a}\left(\frac{h}{(w+N_1)^2}-\frac{1}{K}\right) \end{bmatrix} w_1,$$

so that we obtain $w_1 = 1$ and $w_2 = \frac{r(b+kmA+N_1)}{a}\left(\frac{h}{(w+N_1)^2}-\frac{1}{K}\right)$. Under the condition of weak Allee effect, it follows that $h < \frac{(K+w)^2}{4K}$. Since $h < \frac{(K+w)^2}{4K}$, it can be shown that

$$\frac{r\left(b+kmA+N_1\right)}{a}\left(\frac{h}{\left(w+N_1\right)^2}-\frac{1}{K}\right) < 0.$$

Thus, we get $w_2 < 0$. Furthermore, the corresponding left eigenvector is

$$\vec{v} = \begin{bmatrix} v_1 & v_2 \end{bmatrix},$$

which yields

$$\begin{bmatrix} v_1 & v_2 \end{bmatrix} \begin{bmatrix} rN_1\left(\frac{h}{(w+N_1)^2}-\frac{1}{K}\right) & -\frac{aN_1}{b+kmA+N_1} \\ 0 & 0 \end{bmatrix} = \begin{bmatrix} 0 & 0 \end{bmatrix}.$$

Hence, we obtain $v_1 = 0$ and v_2 is an arbitrary real number. Then, the corresponding left eigenvector can be written as

$$[0 \quad v_2] = [0 \quad 1]\, v_2.$$

By choosing $v_2 = 1$, we get $\vec{v} = [0 \quad 1]$. From model (2), we get

$$\begin{array}{lll} \frac{\partial^2 F_2(E_1,c^*)}{\partial N^2} = 0, & \frac{\partial^2 F_2(E_1,c^*)}{\partial N \partial P} = \frac{c(b+kmA-mA)}{(b+kmA+N_1)^2}, \\ \frac{\partial^2 F_2(E_1,c^*)}{\partial N \partial c} = 0, & \frac{\partial^2 F_2(E_1,c^*)}{\partial P \partial c} = \frac{mA+N_1}{b+kmA+N_1}, \end{array}$$

then Castillo-Chavez and Song theorem [42] gives

$$\begin{aligned} p &= v_2 w_1 w_1 \frac{\partial^2 F_2\left(E_1,c^*\right)}{\partial N^2} + v_2 w_1 w_2 \frac{\partial^2 F_2\left(E_1,c^*\right)}{\partial N \partial P} \\ &= \frac{w_2 c\left(b+(k-1)mA\right)}{\left(b+kmA+N_1\right)^2} \\ &< 0, \\ q &= v_2 w_1 \frac{\partial^2 F_2\left(E_1,c^*\right)}{\partial N \partial c} + v_2 w_2 \frac{\partial^2 F_2\left(E_1,c^*\right)}{\partial P \partial c} \\ &= \frac{w_2(mA+N_1)}{b+kmA+N_1} \\ &< 0. \end{aligned}$$

Thus, the model (1) undergoes a forward bifurcation at $c = c^*$. □

6.2. Hopf Bifurcation

Furthermore, the existence of a Hopf bifurcation is established in Theorem 13.

Theorem 13. *Let* $N_4 = \frac{\delta(b+kmA)-cmA}{c-\delta}$ *and* $P_4 = \frac{r(b+kmA+N_4)\left[(K-w)N_4-K(h-w)-N_4^2\right]}{Ka(w+N_4)}$. *If condition of Theorem 5 is satisfied and* $w \neq b+kmA$, *then a Hopf bifurcation occurs at the value* $h = h^*$, *where*

$$h^* = \frac{(w+N_4)^2(b+kmA+2N_4-K)}{K(b+kmA-w)}.$$

Proof. The Jacobian matrix at $E_4\left(N_4, P_4\right)$ is given by

$$J_{E_4} = \begin{bmatrix} \left(\frac{Kh-(w+N_4)^2}{K(w+N_4)^2}\right) rN_4 + \frac{aN_4P_4}{(b+kmA+N_4)^2} & -\frac{aN_4}{b+kmA+N_4} \\ \frac{(b+kmA-mA)cP_4}{(b+kmA+N_4)^2} & 0 \end{bmatrix}. \tag{17}$$

From the Jacobian matrix (17), we get the characteristic equation as follows:

$$\lambda^2 - \operatorname{tr}\left(J_{E_4}\right)\lambda + \det\left(J_{E_4}\right) = 0. \tag{18}$$

with

$$\begin{aligned} \operatorname{tr}\left(J_{E_4}\right) &= \frac{(w+N_4)^2(K-b-kmA-2N_4)}{(w+N_4)^2(b+kmA+N_4)} \\ &\quad + \frac{Kh(b+kmA-w)}{(w+N_4)^2(b+kmA+N_4)} \times \frac{rN_4}{K}, \\ \det\left(J_{E_4}\right) &= \frac{ac(b+(k-1)mA)N_4P_4}{(b+kmA+N_4)^3} > 0. \end{aligned}$$

Using the characteristic eq. (18), the eigenvalue λ is determined as

$$\lambda_{1,2} = \frac{1}{2}\left(\operatorname{tr}\left(J_{E_4}\right) \pm \sqrt{\operatorname{tr}\left(J_{E_4}\right)^2 - 4\det\left(J_{E_4}\right)}\right).$$

If $h = h^*$ where

$$h^* = \frac{(w+N_4)^2(b+kmA+2N_4-K)}{K(b+kmA-w)},$$

then it can be shown that $\operatorname{tr}\left(J_{E_4}\right) = 0$. Since $\det\left(J_{E_4}\right) > 0$, eigenvalues $\lambda_{1,2}$ are pure imaginer.

Now, we verify the transversality condition. The transversality condition of the Hopf bifurcation is expressed as follows:

$$\frac{d\operatorname{Re}(\lambda)}{dh}\Big|_{h=h^*} = \frac{KrN_4(b+kmA-w)}{K(w+N_4)^2(b+kmA+N_4)}.$$

If $w \neq b+kmA$, then $\frac{d\operatorname{Re}(\lambda)}{dh}\Big|_{h=h^*} \neq 0$. As the result, a Hopf bifurcation occurs at $h = h^*$. □

7. Numerical Simulation

In this section, we carry out a numerical study of the dynamic behavior of the model (1) to complement the above analytical results. Numerical simulations are carried out to illustrate the local and global stability, as well as forward and Hopf bifurcation, in the presence of the Allee effect. We used hypothetical data to match the conditions in the analytical findings, as there were no available field data.

7.1. Global Stability

The first simulation is performed to show the global dynamics of the model (1), which is affected by the Allee effect. Analytically, model (1), under the influence of the weak Allee effect, has two globally asymptotically stable equilibrium points, namely

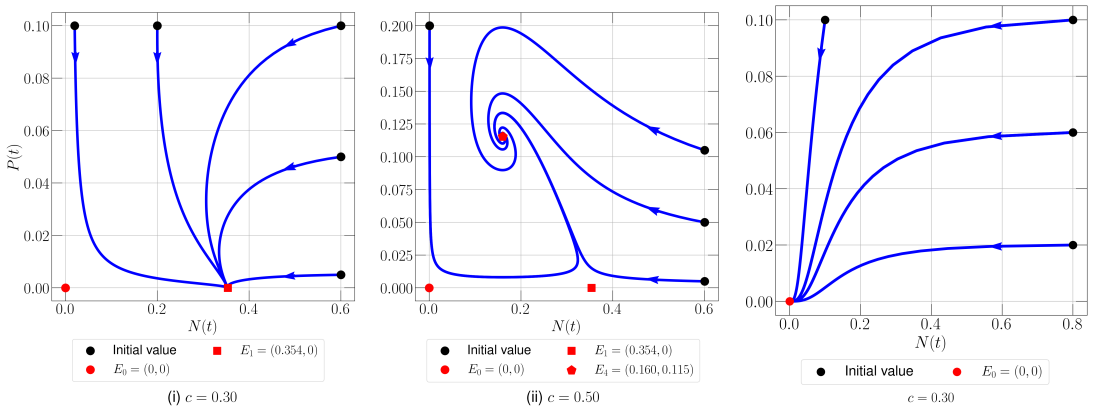

(a) under a weak Allee effect

(b) under a strong Allee effect

Figure 1. Phase portrait showing global stability of the model (1).

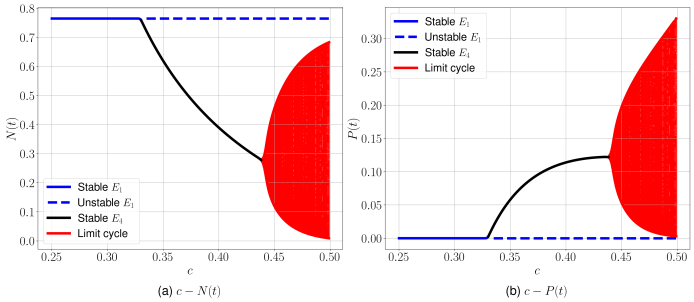

Figure 2. Forward and Hopf bifurcation diagrams of the model (1) under a weak Allee effect $(h < w)$.

Table 2. Parameter values to indicate global stability under the influence of weak Allee effect.

Parameter	r	K	h	w	a	b	δ	k	m	A
Value	0.2	0.5	0.25	0.5	0.6	0.9	0.2	0.3	0.5	0.6

the semi-trivial point (E_1) with the stability conditions stated in Theorem 10, and the interior point (E_4) with the stability conditions stated in Theorem 11. To demonstrate the dynamics, the parameter values in Table 2 are used by choosing $c = 0.30$ and $c = 0.50$, which satisfy the global stability condition. The dynamics are illustrated in the phase portrait in Figure 1a.

The phase portrait in Figure 1a illustrates the global stability of the semi-trivial point E_1 and the interior point E_4 under the weak Allee effect $(h < w)$. In Figure 1a (i) with $c = 0.3$, there are two equilibrium points that exist: the trivial point $E_0(0,0)$, which is unstable, and the semi-trivial point $E_1(0.354,0)$, which is globally asymptotically stable. This condition indicates the extinction of the predator, while the prey can survive. When the predation conversion rate is increased to $c = 0.5$ as shown in Figure 1a (ii), there are three equilibrium points that exist, each of which is the trivial point $E_0(0,0)$ and the axial point $E_1(0.354,0)$ which is unstable, as well as the interior point $E_4(0.160,0.115)$ which is globally asymptotically stable. This condition indicates that both predator and prey populations can survive in the long term.

Additionally, it can be demonstrated that the model (1), affected by the strong Allee effect, has one stable equilibrium point, which is the trivial point E_0, following the stability condition outlined in Theorem 9. To show how the system behaves, we use the parameter values from Table 3 that meet the global stability condition, and we display those values in the phase portrait in Figure 1b.

Figure 1b shows that the equilibrium point $E_0(0,0)$ is the only point that exists and is globally asymptotically stable. The evidence indicates that a strong Allee effect could lead to the extinction of both populations. However, by increasing the carrying capacity of the environment (K), there is potential for both populations to survive in the long term. This condition is further explored numerically in the next section. We perform local numerical exploration around the equilibrium point to identify more complex dynamics in the model (1). We selected the parameter values in this simulation based on local stability conditions. The parameters include the predation conversion rate (c), the environmental protection rate (b), and the quantity of supplementary food for predators (A), which can mathematically influence the stability of the equilibrium point.

7.2. *Influence of Predation Conversion Rate*

In this section, numerical simulations are performed using parameter values that satisfy the local stability conditions, namely $K = 1.0$, $w = 0.3$, and the remaining parameter values as given in Table 2. According to Theorem 12, a forward bifurcation point is obtained at $c \approx 0.329$, and according to Theorem 13,

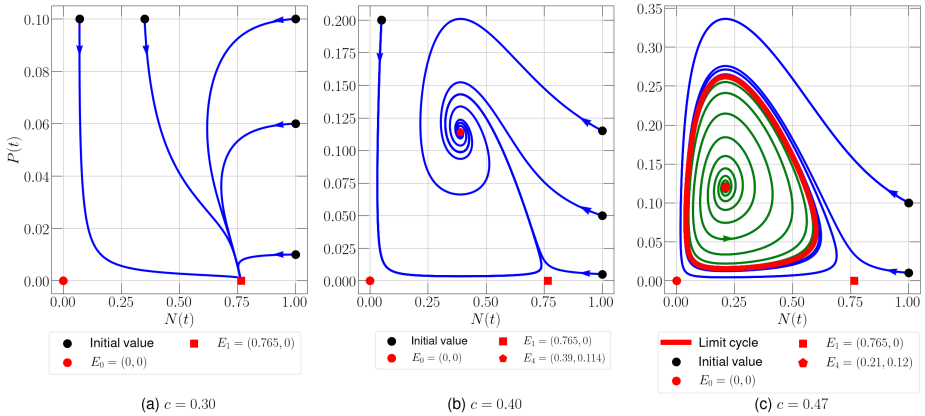

(a) $c = 0.30$ (b) $c = 0.40$ (c) $c = 0.47$

Figure 3. The phase portrait with a weak Allee effect $(h < w)$ shows that an increase in the predation conversion rate causes a transition from predator extinction to oscillatory behavior in both populations.

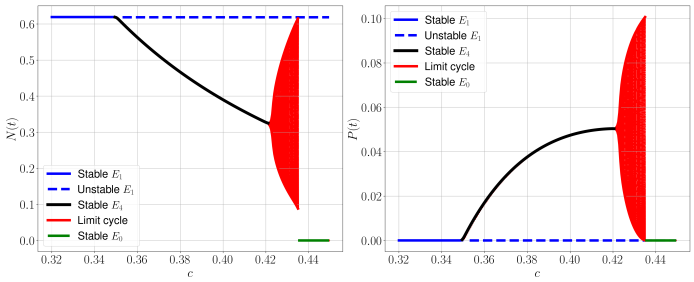

(a) $c - N(t)$ (b) $c - P(t)$

Figure 4. Forward and Hopf bifurcation diagrams of the model (1) under a strong Allee effect $(h > w)$.

Table 3. Parameter values to indicate global stability under the influence of strong Allee effect.

Parameter	r	K	h	w	a	b	c	δ	k	m	A
Value	0.2	0.29	0.35	0.3	0.6	0.9	0.3	0.2	0.3	0.5	0.6

a Hopf bifurcation point is obtained at $c \approx 0.439$. Therefore, the range $c \in [0.25, 0.50]$ is considered to investigate the effect of increasing the predation conversion rate c on the qualitative behavior of the solutions of model (1), with the corresponding bifurcation diagram shown in Figure 2.

The bifurcation diagram in Figure 2 illustrates the dynamic behavior of the model with two bifurcation points: $c_1^* \approx 0.329$, indicating a forward bifurcation, and $c_2^* \approx 0.439$, marking a Hopf bifurcation. For the predation conversion rate in the interval $0 \leq c < c_1^*$, there is local stability at the semi-trivial point E_1, which becomes unstable when $c > c_1^*$. In the interval $c_1^* < c < c_2^*$, local stability shifts to the interior point E_4, which also becomes unstable after $c > c_2^*$, accompanied by the emergence of a limit cycle. These phenomena indicate that increasing the predation conversion rate leads to forward and Hopf bifurcations. To examine the model's dynamic behavior under weak Allee effects, several values of the predation conversion rate, specifically $c = 0.13, 0.40$, and 0.47, are selected, as depicted in the phase portrait in Figure 3.

The phase portraits in Figure 3 illustrate the dynamic behavior of predator-prey systems influenced by the predation conversion rate under weak Allee effects. In Figure 3a with $c = 0.30$, two equilibrium points exist: the unstable trivial point $E_0(0, 0)$ and the locally stable semi-trivial point $E_1(0.765, 0)$, indicating predator extinction while the prey survives. Figure 3b, with $c = 0.40$, shows three equilibrium points: the unstable E_0, the unstable E_1, and the locally stable interior point $E_4(0.39, 0.114)$, suggesting both populations can persist long-term without oscillations. In Figure 3c, with $c = 0.47$, all three equilibrium points become unstable, but a limit cycle arises around E_4, indicating long-term survival with oscillations. Thus, increasing the predation conversion rate (c) may enhance stability between predator and prey, but excessive increases lead to regular fluctuations. As prey increases, predator populations rise due to ample food, but increased predation subsequently reduces prey numbers, creating a continuous cycle of fluctuations.

Furthermore, the model with a strong Allee effect shows global stability at the trivial point E_0 as shown in Figure 1b. Parameter values satisfying local stability conditions, specifically $K = 1.0$ and those in Table 3, are chosen to see more complex dynamics. By choosing an appropriate value of $c \in [0.33, 0.43]$ and a suitable initial value, the effect of increasing the predation conversion rate (c) on the solution of the model (1) with a strong Allee effect can be observed through the bifurcation diagram in Figure 4.

The bifurcation diagram in Figure 4 illustrates the local dynamical behavior of the model, with bifurcation points at $c_1^* \approx 0.35$ for forward bifurcation and $c_2^* \approx 0.422$ for Hopf bifurcation. For predation conversion rates in the interval $0 \leq c < c_1^*$, local stability is observed at the semi-trivial point E_1, which becomes unstable when $c > c_1^*$. Between c_1^* and c_2^*, stability shifts to the interior point E_4, becoming unstable beyond c_2^* and result-

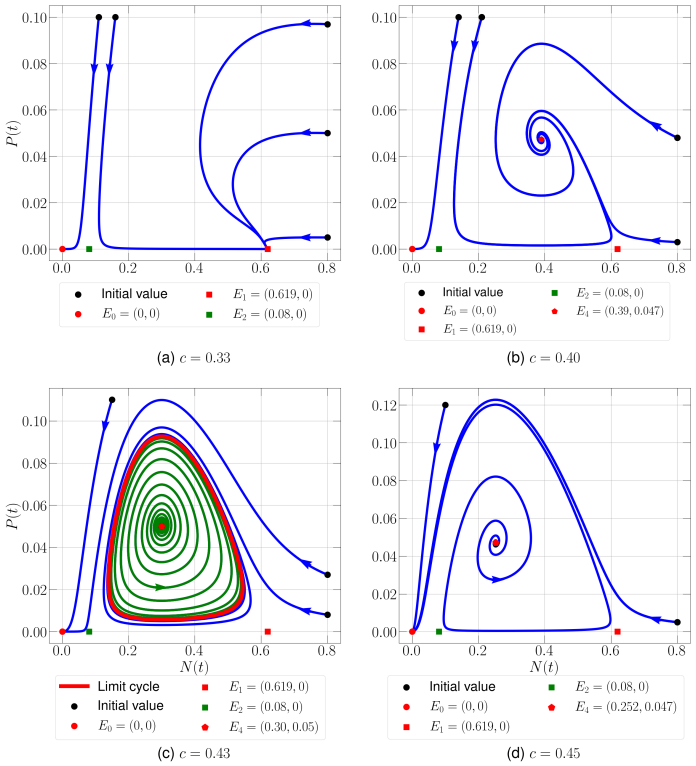

Figure 5. The phase portrait with a strong Allee effect $(h > w)$ shows that an increase in the predation conversion rate causes a transition from predator extinction to oscillatory behavior in both populations, potentially leading to the extinction of both.

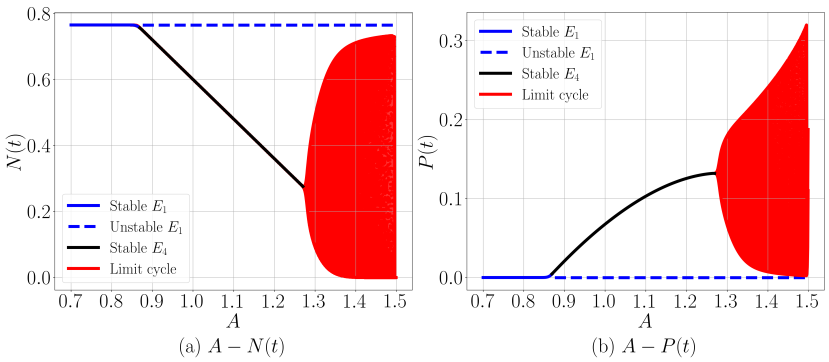

Figure 6. Forward and Hopf bifurcation diagrams of the model (1) under a weak Allee effect $(h < w)$.

ing in a limit cycle. As the predation conversion rate increases, both forward and Hopf bifurcations occur. However, if c exceeds 0.435, the system loses the limit cycle phenomenon and achieves local stability at the trivial point E_0. To analyze the model's behavior under a strong Allee effect, several predation conversion rates, specifically $c = 0.33, 0.40, 0.43$, and 0.45 are selected, as depicted in the phase portrait in Figure 5.

Figure 5 illustrates the dynamic behavior of predator-prey systems under a strong Allee effect influenced by the predation conversion rate. In Figure 5a with $c = 0.33$, three equilibrium points are present: the locally stable trivial point $E_0(0, 0)$, and two semi-trivial points, $E_1(0.619, 0)$ which is stable, and $E_2(0.08, 0)$ which is unstable. Figure 5b-d for $c = 0.40, 0.43$, and 0.45 show four equilibrium points with varying stability. Specifically, Figure 5b indicates two stable points (E_0 and the interior point $E_4(0.39, 0.047)$) and two unstable points (E_1 and E_2). Figure 5c shows that while E_0 is stable, both E_1 and E_2 are unstable, and $E_4(0.30, 0.05$ loses stability with a limit cycle emerging. In Figure 5d, E_0 emerges as the only stable point while the other three equilibria become unstable.

These conditions indicate bistability, depending on the initial conditions shown in Figure 5a-c. If the initial conditions are below a threshold, the model solution converges to E_0, leading to population extinction. On the other hand, it converges to a distinct equilibrium above the threshold. The solution converges to E_1 at $c = 0.33$, suggesting that the prey survives while the predator extinction occurs. Both populations can coexist without oscillation at $c = 0.40$, suggesting a stable relationship. However, regular fluctuations are caused by the loss of stability in E_4 at $c = 0.43$. Ultimately, the model converges to E_0 when c approaches 0.45, indicating the extinction of both populations. This suggests that excessively high predation conversion rates can destabilize the ecosystem and lead to population extinction.

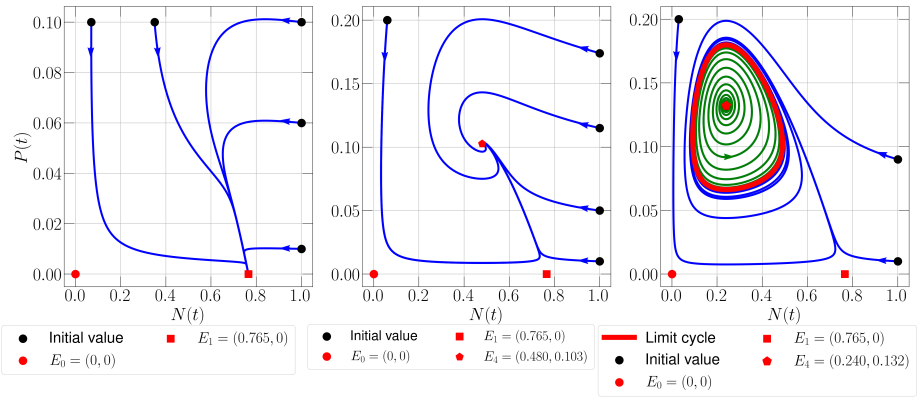

(a) $A = 0.80$ (b) $A = 1.10$ (c) $A = 1.30$

Figure 7. The phase portrait with a weak Allee effect $(h < w)$ indicates that an increase in the quantity of supplementary food for the predator causes a transition from predator extinction to oscillatory behavior in both populations.

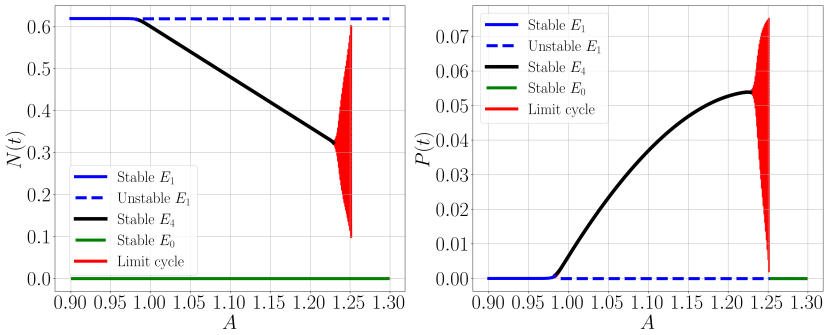

(a) $A - N(t)$ (b) $A - P(t)$

Figure 8. Forward and Hopf bifurcation diagrams of the model (1) under a strong Allee effect $(h > w)$.

Overall, the Allee effect and predation conversion rate have a complex impact on population dynamics when combined. A weak Allee effect can cause population oscillations by pushing the system from extinction to stable coexistence through an increase in the rate of predation conversion. On the other hand, a high rate of predation conversion combined with a strong Allee effect can cause population extinction because it destabilizes the system.

7.3. Influence of the Quantity of Predator Supplementary Food

In this section, simulations are carried out by selecting parameter values that satisfy the local stability conditions, namely $K = 1.0, w = 0.3, c = 0.3$, and the other parameter values listed in Table 2. According to Theorem 12, a forward bifurcation point is obtained at $A = 0.862$, and according to Theorem 13, a Hopf bifurcation point is obtained at $A = 1.279$. Therefore, the value of $A \in [0.70, 1.50]$ is used to observe the effect of the quantity of predator supplementary food (A) on the behavior of the solution of model (1), with the corresponding bifurcation diagram shown in Figure 6.

Figure 6 illustrates the model's behavior with two bifurcation points: $A_1^* \approx 0.862$ for forward bifurcation and $A_2^* \approx 1.279$ for Hopf bifurcation. The quantity of supplementary food for predators is stable at the semi-trivial point E_1 for $0 \leq A < A_1^*$ and loses stability when $A > A_1^*$. Local stability then shifts to the interior point E_4 in the interval $A_1^* < A < A_2^*$, after which instability leads to the emergence of a limit cycle when $A > A_2^*$. This indicates that both forward and Hopf bifurcations occur with increasing supplementary food for predators. The quantities of supplementary food selected for various intervals, specifically $A = 0.8, 1.1$, and 1.3 demonstrate the model's dynamic behavior with a weak Allee effect, as seen in the phase portraits in Figure 7.

The phase portrait in Figure 7 illustrates the dynamic behavior of the predator-prey system influenced by supplementary food for predators under weak Allee effects. In Figure 7a with $A = 0.8$, two equilibrium points are present: the unstable trivial point E_0 and the asymptotically stable semi-trivial point E_1, indicating predator extinction while prey survives. Figure 7b with $A = 1.1$ shows three equilibrium points: E_0 (unstable), E_1 (unstable), and the stable interior point E_4, suggesting that both populations can survive long-term without oscillation. In Figure 7c with $A = 1.3$, all three points become unstable, but a limit cycle emerges around E_4, suggesting that both populations can survive with oscillatory behavior. This indicates that increasing the quantity of supplementary food for the predators may promote stability between species, with populations stabilizing at a certain level. However, higher supplementary food for the predators can lead to regular fluctuations, as increased food leads to increased predator numbers, which then reduce the prey population, creating a continuous cycle of fluctuations.

Furthermore, the model (1) with a strong Allee effect shows global stability at the trivial point E_0, as shown in Figure 1b. Parameter values satisfying local stability conditions, specifically $K = 1.0$ and those in Table 3, are chosen to see more complex dynamics. By choosing $A \in [0.90, 1.30]$ and suitable initial val-

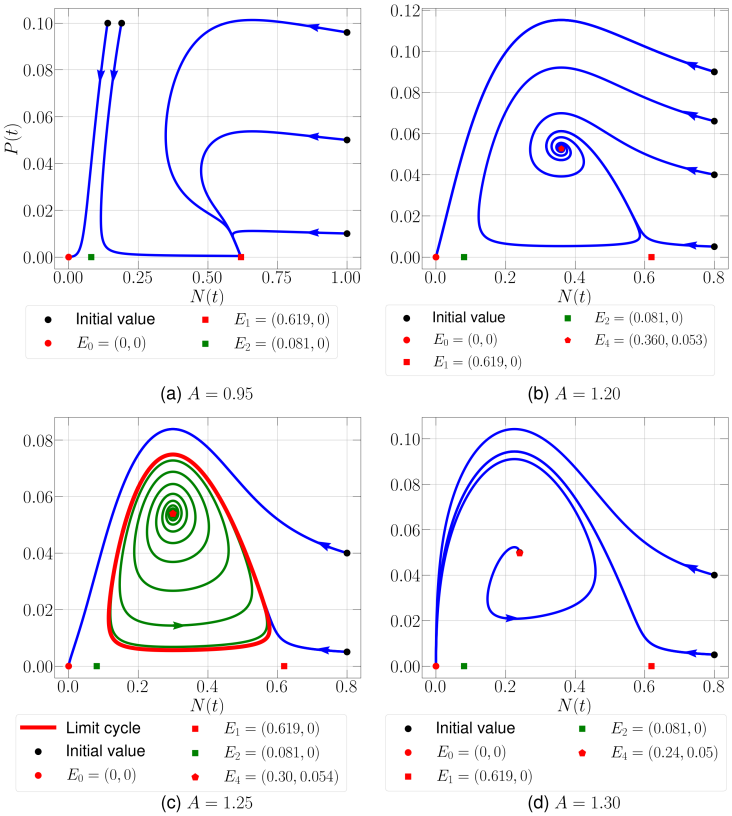

Figure 9. The phase portrait with a strong Allee effect $(h > w)$ indicates that an increase in the quantity of supplementary food for the predator causes a transition from predator extinction to oscillatory behavior in both populations, potentially leading to extinction in both.

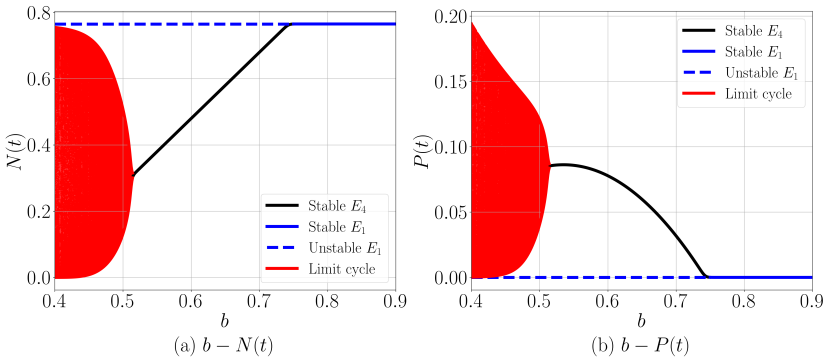

Figure 10. Forward and Hopf bifurcation diagrams of model (1) under a weak Allee effect $(h < w)$.

ues, the impact of increasing supplementary food for predators (A) on the model's solutions can be analyzed using the bifurcation diagram in Figure 8.

Figure 8 shows the local dynamics of the model (1), highlighting two bifurcation points: $A_1^* \approx .0.984$ for forward bifurcation and $A_2^* \approx .1.235$ for Hopf bifurcation. In the range $0 \leq A < A_1^*$, stability occurs at the semi-trivial point E_1, which becomes unstable for $A > A_1^*$. Between $A_1^* < A < A_2^*$, local stability shifts to the interior point E_4 until $A > A_2^*$, when a limit cycle emerges. This indicates the occurrence of both bifurcations as supplementary food for predators increases. If A exceeds 1.25, the system loses the limit cycle and stabilizes at the trivial point E_0. To illustrate the model's dynamics with a strong Allee effect, several supplementary food values are selected: $A = 0.95, 1.20, 1.25,$ and 1.30, as shown in the phase portrait in Figure 9.

Figure 9 illustrates the dynamics of the predator-prey system influenced by supplementary food under strong Allee effects. In Figure 9a with $A = 0.95$, three equilibrium points exist: the asymptotically stable trivial point E_0, the stable semi-trivial point E_1, and the unstable semi-trivial point E_2. Figure 9b to Figure 9d with $A = 1.20, 1.25,$ and 1.30 show four equilibrium points with varying stability: E_0, the interior point E_4, and the semi-trivial points E_1 and E_2. In Figure 9b ($A = 1.20$), E_0 and E_4 are stable, while E_1 and E_2 are unstable. Figure 9c ($A = 1.25$) displays E_0 as stable, while E_1, E_2, and E_4 are unstable, with a limit cycle present. Finally, Figure 9d ($A = 1.30$) shows E_0 as the only stable equilibrium, with the other points unstable.

This condition indicates bistability, depending on initial conditions, as shown in Figure 9a to Figure 9c. If the initial con-

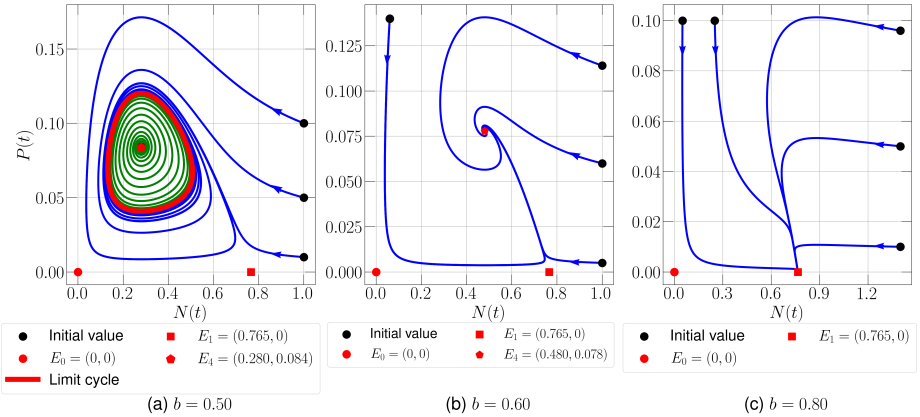

(a) $b = 0.50$ (b) $b = 0.60$ (c) $b = 0.80$

Figure 11. The phase portrait with a weak Allee effect $(h < w)$ shows that an increase in the environmental protection rate causes a transition from an oscillatory behavior in both populations to predator extinction.

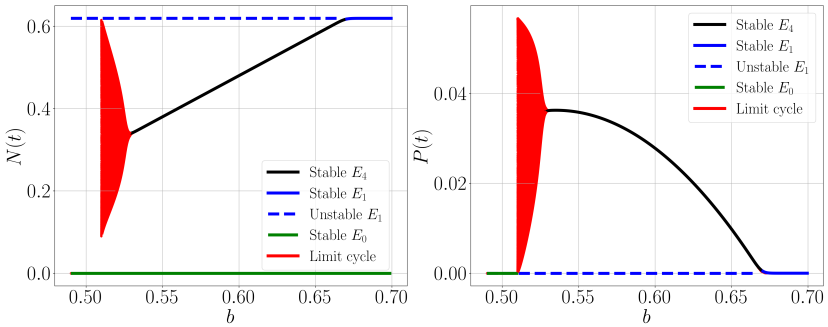

(a) $b - N(t)$ (b) $b - P(t)$

Figure 12. Forward and Hopf bifurcation diagrams of the model (1) under a strong Allee effect $(h > w)$.

ditions are below a certain threshold, the solution to the model (1) converges to E_0, leading to the extinction of both populations. On the other hand, should the starting conditions surpass this limit, the solution converges to points apart from E_0. For $A = 0.95$, the solution converges to E_1, showing that predators go extinct while prey survives. For $A = 1.2$, the model converges to E_4, indicating both populations can persist long-term without oscillations, demonstrating a stable predator-prey relationship. However, increasing A to 1.25 causes E_4 to lose stability and results in a limit cycle, where both populations fluctuate regularly. When A reaches 1.3, the solution converges to E_0, indicating complete extinction. These findings suggest that excessive supplementary food for predators may disrupt ecosystem balance and lead to population decline or extinction.

Overall, the stability and viability of populations are impacted by the Allee effect and the quantity of supplementary food for predators. Increased supplementary food sources foster the shift from extinction to coexistence and ultimately to oscillatory behavior under a weak Allee effect. On the other hand, too much supplementary food accelerates system imbalance and raises the possibility of population extinction under the strong Allee effect.

7.4. Influence of Environmental Protection Rate

In this section, simulations are carried out by selecting parameter values that meet the local stability conditions, namely $K = 1.0$, $w = 0.3$, $c = 0.3$, and other parameter values in Table 2. A value of $b \in [0.40, 0.90]$ is used to observe the effect of increasing the environmental protection rate (b) on the behavior of the model (1) solution, with the bifurcation diagram in Figure 10.

The bifurcation diagram in Figure 10 illustrates three dynamic behaviors of the model with two bifurcation points: $b_1^* \approx 0.512$ indicating a Hopf bifurcation and $b_2^* \approx 0.743$ indicating a forward bifurcation. In the interval $0 \leq b < b_1^*$, a limit cycle phenomenon is observed around the interior point E_4. As the environmental protection rate increases within the range $b_1^* < b < b_2^*$, the limit cycle phenomenon and local stability at E_4 are lost. When $b > b_2^*$, the interior point becomes unstable and shifts to the semi-trivial point E_1, marking the occurrence of both Hopf and forward bifurcations based on changes in the environmental protection rate. To illustrate the model's dynamic behavior with a weak Allee effect, several environmental protection rate values, specifically $b = 0.50, 0.60$, and 0.80 are chosen, as shown in the phase portraits in Figure 11.

Under weak Allee effects, the phase portraits in Figure 11 show the dynamic behavior of the predator-prey system shaped by the environmental protection rate. In Figure 11a with $b = 0.50$, three equilibrium points are identified: the unstable trivial point E_0, the unstable semi-trivial point E_1, and the unstable interior point E_4, with a limit cycle present around E_4. This suggests that consistent behavior allows both populations to survive long-term. With $b = 0.60$, the equilibrium points in Figure 11b comprise the unstable E_0 and E_1, while the interior point E_4 is now locally stable, permitting both populations to exist without oscillations. With $b = 0.80$, only the unstable E_0 and the stable E_1 exist in Figure 11c, suggesting predator extinction while

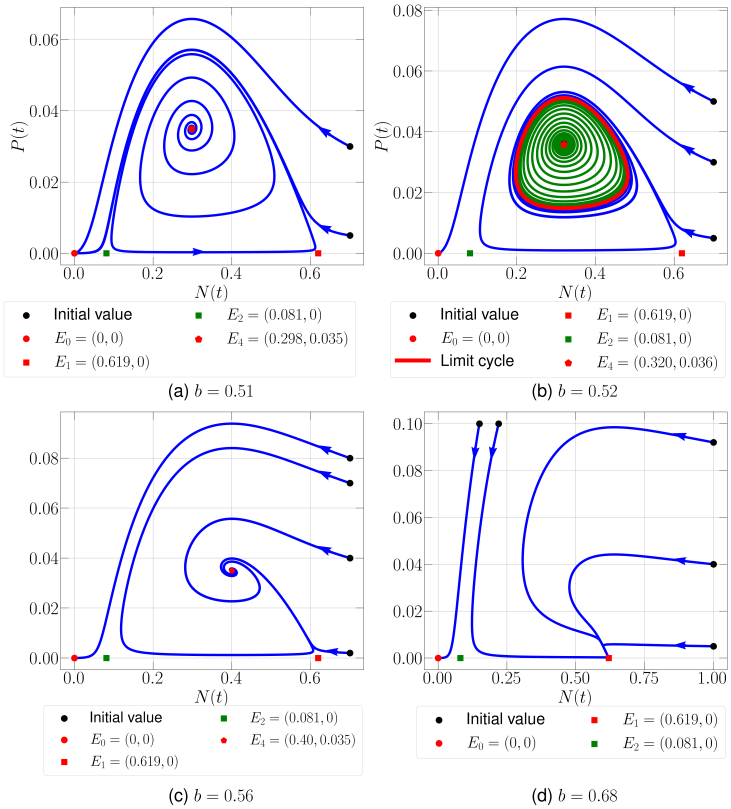

Figure 13. The phase portraits with strong Allee effects ($h > w$) inandicate the potential extinction of both populations, extinction of the predator, or an oscillatory behavior in both populations, depending on changes in the environmental protection rate.

the prey population survives. This implies that at lower rates of environmental protection, both populations show normal oscillations. Increased food availability causes predator populations to rise as prey numbers rise; yet, this finally results in a drop in prey numbers and a following drop in predator populations, therefore generating a cycle. With higher environmental protection rates, prey survival improves, leading to potential predator extinction while the prey continues to survive.

Furthermore, the model with a strong Allee effect shows global stability at the trivial point E_0 as shown in Figure 1b. By choosing the value of $b \in [0.49, 0.70]$ and appropriate initial values, the effect of increasing the environmental protection rate (b) on the solution of the model (1) with a strong Allee effect can be observed through the bifurcation diagram in Figure 12.

The bifurcation diagram in Figure 12 shows the local dynamic behavior of the model (1) with two bifurcation points: $b_1^* \approx 0.525$, indicating a Hopf bifurcation, and $b_2^* \approx 0.669$, indicating a forward bifurcation. A relatively low environmental protection rate ($b < 0.51$) indicates local stability at the trivial point E_0. Increasing the protection rate within the interval $0.51 \leq b < b_1^*$ leads to a limit cycle phenomenon around the interior point E_4. When b falls between b_1^* and b_2^*, the limit cycle and local stability of E_4 are lost. Beyond b_2^*, the interior point becomes unstable and shifts to the semi-trivial point E_1, indicating potential population extinction at low protection rates and the occurrence of both bifurcations. To illustrate the model's dynamic behavior under a strong Allee effect, several environmental protection rate values, specifically $b = 0.50, 0.52, 0.56$, and 0.68, are selected, as depicted in the phase portrait in Figure 13.

Figure 13 shows the dynamic behavior of predator-prey systems influenced by environmental protection rates under strong Allee effects. In Figure 13a-c with $b = 0.51, 0.52$, and 0.56, four equilibrium points are identified: the trivial point E_0, the interior point E_4, and two semi-trivial points E_1 and E_2. In Figure 13a ($b = 0.51$), the only asymptotically stable point is $E_0(0, 0)$, while the other points are unstable. In Figure 13b ($b = 0.52$), E_0 remains stable, alongside unstable points E_1, E_2, and the unstable $E_4(0.32, 0.036$ with a limit cycle. Figure 13c ($b = 0.56$) reveals two stable points, E_0 and $E_4(0.40, 0.035)$, and two unstable points, E_1 and E_2. Figure 13d ($b = 0.68$) shows three equilibrium points: E_0 and E_1 as stable, while E_2 is unstable.

These scenarios imply the possible extinction of both populations when environmental protection is not sufficient, as poor protection for prey causes an increased predation by predators. Furthermore, the extinction of the prey will cause the predator to become extinct, as there is not enough food to survive. Increased environmental protection, however, leads to bistability, which means stability relies on starting conditions, as indicated in Figure 13b-d. The model converges to E_0 if initial conditions fall below a certain threshold, indicating total population extinction. In contrast, if initial conditions exceed the threshold, the solution converges to other equilibrium points. For $b = 0.52$, a limit cycle emerges around the interior point E_4, demonstrating regular fluctuations in both populations. When there is more prey, there is more food for predators, but when there are more predators, there is less prey. At $b = 0.56$, the limit cycle goes away, which means that both populations can live for a long time without oscillations. This evidence shows that the link between

the predator and prey is stable, with few changes. But when protection rates are much higher, like when $b = 0.68$, the model converges to E_1, which means the predators become extinct while the prey survive long-term. This result shows that environmental protection is just enough to keep the population in balance, but protecting it too much could cause predators to go extinct.

Overall, the Allee Effect and the environmental protection rate mutually influence the stability of ecosystem predator-prey relationships. In the weak Allee effect, increased environmental protection can change population dynamics from oscillatory fluctuations to stable coexistence, eventually leading to predator extinction if protection is too high. While in the strong Allee effect, the system becomes more vulnerable, where too low or excessive protection can increase the probability of complete extinction or cause only the prey to survive.

8. Conclusion

We have developed a predator-prey model by integrating the Allee effect on the share and additional food sources for predators. The existence and uniqueness of solutions, as well as their positive and boundedness, prove the validity of this model. Three equilibrium points have been identified: a trivial point indicating the extinction of both populations, a semi-trivial point indicating the extinction of the predator while the prey survives, and an interior point indicating the coexistence of both populations. The strength of the Allee effect and certain parameter conditions affect the local stability of each equilibrium point. In addition, the global stability of each equilibrium point is also demonstrated, providing an overview of the system dynamics in the long term. The analysis shows the presence of Hopf bifurcation and forward bifurcation, which signify the transition of dynamic behavior in the system. Forward bifurcations signify a change in stability that depends on changes in parameter values, while Hopf bifurcations indicate a shift in the stability of the equilibrium point from stable to unstable, leading to the appearance of limit cycles. Numerical simulations support the analytical results by showing how changes in predation conversion rate, environmental protection rate, and the quantity of supplementary food for predators affect the stability of the system. The predator population can survive under weak Allee effect conditions if the predation conversion rate and the availability of supplementary food remain within certain limits, although the prey population remains stable. An increase in the amount of additional food for predators causes a transition from predator extinction to an oscillatory pattern of both populations. In contrast, under strong Allee effect conditions, the simulations show greater complexity, where an increase in predation conversion rate can result in a transition from predator extinction to oscillatory behavior, and if the predation rate is too high, both species could potentially go extinct. These results support the idea that significant Allee effects can exacerbate population resilience to environmental change, which is relevant for better management and conservation plans.

Author Contributions. **Resmawan, R.**: Conceptualization, Formal analysis and investigation, Writing - original draft preparation, Resources. **Suryanto, A.**: Conceptualization, Formal analysis and investigation, Writing - review and editing, Supervision. **Darti, I.**: Conceptualization, Formal analysis and investigation, Writing - review and editing, Supervision. **Panigoro, H. S.**: Conceptualization, Formal analysis and investigation, Writing - review and editing, Supervision.

Acknowledgement. The authors are thankful to the Department of Mathematics, Faculty of Mathematics and Natural Sciences, University of Brawijaya, for providing academic and technical support during this research. The authors also express gratitude to the editors and reviewers who have contributed to improving the quality of this article.

Funding. This work was supported by the Ministry of Higher Education, Science, and Technology of the Republic of Indonesia through the Center for Higher Education Funding and Assessment (PPAPT) and the Indonesia Endowment Fund for Education (LPDP), which provided the Indonesian Education Scholarship (BPI-Beasiswa Pendidikan Indonesia).

Conflict of interest. The authors declare no potential conflict of interests.

Data availability. Not applicable.

Abbreviations.

L.A.S	:	Locally Asymptotically Stable
G.A.S	:	Globally Asymptotically Stable

References

[1] A. J. Lotka, "Elements of physical biology," *Science Progress in the Twentieth Century (1919-1933)*, vol. 21, no. 82, pp. 341–343, 1926.

[2] V. Volterra, *Variazioni e fluttuazioni del numero d'individui in specie animali conviventi*. Società Anonima Tipografica "Leonardo da Vinci", 1927.

[3] G. F. Gause, N. P. Smaragdova, and A. A. Witt, "Further studies of interaction between predators and prey," *Journal of Animal Ecology*, vol. 5, no. 1, pp. 1–18, 1936. DOI:10.2307/1087

[4] X. Chen and X. Zhang, "Dynamics of the predator-prey model with the sigmoid functional response," *Studies in Applied Mathematics*, vol. 147, no. 1, pp. 300–318, 2021. DOI:10.1111/sapm.12382

[5] W. Su and X. Zhang, "Predator–prey model with sigmoid functional response," *Studies in Applied Mathematics*, vol. 152, no. 3, pp. 868–902, 2024. DOI:10.1111/sapm.12667

[6] C. S. Holling, "Some characteristics of simple types of predation and parasitism," *The Canadian Entomologist*, vol. 91, no. 7, pp. 385–398, 1959. DOI:10.4039/Ent91385-7

[7] C. S. Holling, "The functional response of predators to prey density and its role in mimicry and population regulation," *Memoirs of the Entomological Society of Canada*, vol. 97, no. S45, pp. 5–60, 1965. DOI:10.4039/entm9745fv

[8] F. Liu and F. Wei, "An epidemic model with beddington-deangelis functional response and environmental fluctuations," *Physica A: Statistical Mechanics and its Applications*, vol. 597, p. 127321, 2022. DOI:10.1016/j.physa.2022.127321

[9] Z. Liang and X. Meng, "Stability and hopf bifurcation of a multiple delayed predator-prey system with fear effect, prey refuge and crowley-martin function," *Chaos, Solitons & Fractals*, vol. 175, p. 113955, 2023. DOI:10.1016/j.chaos.2023.113955

[10] X. Chen and W. Yang, "Impact of fear-induced group defense in a monod–haldane type prey–predator model," *Journal of Applied Mathematics and Computing*, vol. 70, pp. 3331–3368, 2024. DOI:10.1007/s12190-024-02101-8

[11] J. Gascoigne, L. Berec, S. D. Gregory, and F. Courchamp, , "Dangerously few liaisons: a review of mate-finding allee effects," *Population Ecology*, vol. 51, no. 3, pp. 355–372, 2009. DOI:10.1007/s10144-009-0146-4

[12] E. Rahmi *et al.*, "Stability analysis of a fractional-order leslie-gower model with allee effect in predator," in *Journal of Physics: Conference Series*, vol. 1821, p. 012051, 2021. DOI:10.1088/1742-6596/1821/1/012051

[13] H. S. Panigoro and E. Rahmi, "Computational dynamics of a lotka-volterra model with additive allee effect based on atangana-baleanu fractional derivative," *Jambura Journal of Biomathematics (JJBM)*, vol. 2, no. 2, pp. 96–103, 2021. DOI:10.34312/jjbm.v2i2.11886

[14] H. S. Panigoro and E. Rahmi, "Impact of fear and strong allee effects on the dynamics of a fractional-order rosenzweig-macarthur model," in *Springer Proceedings in Complexity, International Conference on Nonlinear Dynamics and*

Applications (ICNDA 2022), 2022. DOI:10.1007/978-3-030-99792-2_50 pp. 611–619.

[15] E. Rahmi, I. Darti, A. Suryanto, and T. Trisilowati, "A modified leslie-gower model incorporating beddington-deangelis functional response, double allee effect, and memory effect," *Fractal and Fractional*, vol. 5, no. 3, p. 84, 2021. DOI:0.3390/fractalfract5030084

[16] N. Anggriani *et al.*, "A predator-prey model with additive allee effect and intraspecific competition on predator involving atangana-baleanu-caputo derivative," *Results in Physics*, vol. 49, p. 106489, 2023. DOI:10.1016/j.rinp.2023.106489

[17] F. Wang and R. Yang, "Dynamics of a delayed reaction–diffusion predator–prey model with nonlocal competition and double allee effect in prey," *International Journal of Biomathematics*, vol. 18, no. 02, p. 2350097, 2025. DOI:10.1142/S1793524523500973

[18] H. S. Panigoro, E. Rahmi, and O. J. Peter, "Recognizing the complexity of a predator–prey relationship with allee and fear effects in a discrete□time model," in *AIP Conference Proceedings*, vol. 3083, no. 1, p. 050003, 2024. DOI:10.1063/5.0224886

[19] A. Kumar, K. P. Reshma, and H. P. Shri, "Global dynamics of an ecological model in presence of fear and group defense in prey and allee effect in predator," *Nonlinear Dynamics*, vol. 113, pp. 7483–7518, 2025. DOI:10.1007/s11071-024-10706-8

[20] H. S. Panigoro, E. Rahmi, and O. J. Peter, "Recognizing the complexity of a predator-prey relationship with allee and fear effects in a discrete-time model," in *AIP Conference Proceedings*, vol. 3083, no. 1, p. 050003, 2024. DOI:10.1063/5.0224886

[21] P. Luis, P. Z. Kamalia, O. J. Peter, and D. Aldila, "Implementation of non-standard finite difference on a predator-prey model considering cannibalism on predator and harvesting on prey," *Jambura Journal of Biomathematics*, vol. 6, no. 1, 2025. DOI:10.37905/jjbm.v6i1.30550

[22] J. P. Tripathi *et al.*, "Dynamics of a prey-predator model: Untangling the role of fear-induced allee effect, prey refuge, and group defense," *Journal of Biological Systems*, vol. 33, no. 01, pp. 143–194, 2025. DOI:10.1142/S0218339025500019

[23] R. Resmawan, A. Suryanto, I. Darti, and H. S. Panigoro, "Dynamical analysis of a predator-prey model with additive allee effect and prey group defense," *arXiv preprint arXiv:2410.13345*, 2024. DOI:10.48550/arXiv.2410.13345

[24] R. Resmawan, A. Suryanto, I. Darti, and H. S. Panigoro, "Dynamics of a prey-predator model with Allee effects and Holling type IV functional response: local stability and numerical exploration of bifurcations," *Barekeng: Jurnal Ilmu Matematika dan Terapan*, vol. 19, no. 4, pp. 2891–2906, 2025. DOI:10.30598/barekengvol19iss4pp2891-2906

[25] R. Resmawan, A. Suryanto, I. Darti, and H. S. Panigoro, "Global stability and bifurcation analysis of a predator-prey model involving Allee effect and Monod-Haldane functional response," *Mathematical Modelling and Numerical Simulation with Applications*, vol. 5, no. 3, p. Article 3, 2025. DOI:10.53391/2791-8564.1002

[26] R. Kumbhakar, S. Jafari, and N. Pal, "Impacts of predation-driven allee effect and refuge on the dynamics of a predator–prey model in a parameter plane," *International Journal of Bifurcation and Chaos*, vol. 35, no. 03, p. 2550036, 2025.DOI:10.1142/S0218127425500361

[27] M. K. Singh, A. Kumar, and J. Choudhury, "Impact of the allee effect on the dynamics of a predator-prey model exhibiting group defense," *Mathematics*, vol. 13, no. 4, p. 633, 2025. DOI:10.3390/math13040633

[28] R. D. Holt, "Predation, apparent competition, and the structure of prey communities," *Theoretical Population Biology*, vol. 12, no. 2, pp. 197–229, 1977. DOI:10.1016/0040-5809(77)90042-9

[29] S. Debnath, P. Majumdar, S. Sarkar, and U. Ghosh, "Memory effect on prey-predator dynamics: Exploring the role of fear effect, additional food and anti-predator behaviour of prey," *Journal of Computational Science*, vol. 66, p. 101929, 2023. DOI:10.1016/j.jocs.2022.101929

[30] A. Gökçe, "A mathematical modeling approach to analyse the effect of additional food in a predator-prey interactions with a white gaussian noise in prey's growth rate," *International Journal of Applied and Computational Mathematics*, vol. 8, no. 21, 2022. DOI:10.1007/s40819-021-01234-9

[31] K. D. Prasad, B. Prasad, and K. De, "Importance of pesticide and additional food in pest-predator system: a theoretical study," *Journal of Biological Dynamics*, vol. 19, no. 1, pp. 1–19, 2023. DOI:10.1080/17513758.2024.2444263

[32] C. C. García and J. V. Cuenca, "Impact of alternative food on predator diet in a leslie-gower model with prey refuge and holling II functional response," *Mathematical Biosciences and Engineering*, vol. 20, no. 8, pp. 13681–13703, 2023. DOI:10.3934/mbe.2023610

[33] S. Saha, S. Pal, and R. Melnik, "Analysis of the impact of fear in the presence of additional food and prey refuge with nonlocal predator–prey models," *Ecological Modelling*, vol. 505, p. 111103, 2025. DOI:10.1016/j.ecolmodel.2025.111103

[34] S. Mondal and G. Samanta, "Dynamics of an additional food provided predator–prey system with prey refuge dependent on both species and constant harvest in predator," *Physica A: Statistical Mechanics and its Applications*, vol. 534, p. 122301, 2019. DOI:10.1016/j.physa.2019.122301

[35] Y. Wang *et al.*, "Impacts of refuge and additional foods on the spatiotemporal dynamics of a prey-predator system in a time-periodic environment," *European Physical Journal Plus*, vol. 140, p. 330, 2025. DOI:10.1140/epjp/s13360-025-06253-9

[36] M. K. Singh and P. Poonam, "Bifurcation analysis of an additional food-provided predator-prey system with anti-predator behavior," *Mathematical Modelling and Numerical Analysis*, vol. 5, no. 1, pp. 38–64, 2025. DOI:10.53391/mmnsa.1496827

[37] D. Bai and X. Zhang, "Dynamics of a predator-prey model with the additive predation in prey," *Mathematics*, vol. 10, no. 4, p. 655, 2022. DOI:10.3390/math10040655

[38] S. Lynch, "*Dynamical Systems with Applications using Mathematica (1st ed.)*. Boston, MA: Birkhäuser, 2007, ISBN:978-0-8176-4586-1. DOI:10.1007/978-3-319-61485-4

[39] W. N. Li and W. Sheng, "Some gronwall type inequalities on time scales," *Journal of Mathematical Inequalities*, vol. 4, no. 1, pp. 67–76, 2010. DOI:10.1007/s10255-015-0534-9

[40] S. Wiggins, "*Introduction to Applied Nonlinear Dynamical Systems and Chaos (2nd ed.)*." Springer-Verlag New York, vol. 2, 2003. ISBN:978-0-387-00177-7.

[41] M. Martcheva, "*An Introduction to Mathematical Epidemiology (1st ed.)*." New York: Springer, vol. 61, 2015. ISBN 978-1-4899-7611-6 43. DOI:10.1007/978-1-4899-7612-3

[42] C. Castillo-Chavez and B. Song, "Dynamical models of tuberculosis and their applications," *Mathematical Biosciences and Engineering*, vol. 1, no. 2, pp. 361–404, 2004. DOI:10.3934/mbe.2004.1.361